Numerical Analysis and Parametric Study on Multiple Degrees-of-Freedom Frames

George U. Alaneme [1, 2], Alireza Bahrami [3*], Uzoma Ibe Iro [1], Nakkeeran Ganasen [4], Obeten N. Otu [5], Richard C. Udeala [1], Blessing O. Ifebude [1], Emmanuel A. Onwusereaka [1]

[1] *Department of Agricultural Engineering, Michael Okpara University of Agriculture, Umudike, P.M.B. 7267, Umuahia, 440109, Abia, Nigeria.*

[2] *Department of Civil Engineering, Kampala International University, Kampala, Uganda.*

[3] *Department of Building Engineering, Energy Systems and Sustainability Science, Faculty of Engineering and Sustainable Development, University of Gävle, 801 76 Gävle, Sweden.*

[4] *Department of Civil Engineering, SRM Institute of Science and Technology, Kattankulathur, Tamil Nadu, 603203, India.*

[5] *Department of Civil Engineering, University of Cross River State, Calabar, Nigeria.*

Abstract

The design of multiple degrees-of-freedom frames is critical in civil engineering, as these structures are commonly used in various applications such as buildings, bridges, and industrial structures. In this study, a six-degrees-of-freedom beam-column element stiffness matrix was formulated by superposition of beam and truss elements stiffness matrices and was adapted to statically analyze indeterminate frame structures. The development of a numerical model for the frame structures was achieved using the finite element method in the current study. Also, the investigation of the effects of various parameters such as frame geometries, material properties, and loading conditions was conducted on the internal forces developed in the frame structures. Three different parametric study cases that presented the frame structures with varying geometries and loading conditions were analyzed utilizing this matrix approach for the sake of emphasis and to evaluate the flexibility and adequacy of this formula to analyze the indeterminate frames using the MATLAB software. The analysis method comprised the derivation of the system displacements employing the relationships between the stiffness matrix and fixed end forces as the force vector and taking the attained displacements, which would be transformed to the local coordinates to obtain the member forces. The computed results from the element stiffness matrix approach were further statistically compared with the results achieved from the finite element software (SAP2000) applying the analysis of variance (ANOVA). The statistical results showed a P-value > 0.05, which indicated a good correlation between the compared results and adequate performance for the derived beam-column element matrix formula method.

Keywords: Indeterminate Structural Analysis; Beam-Column Element; Analysis of Variance; Matrix Stiffness Method; MATLAB; SAP2000.

1. Introduction

The analysis of multiple degrees-of-freedom (MDOF) frames is vital for designing safe and efficient structures that can withstand various loads and forces. Numerical methods such as the finite element analysis (FEA) and finite difference method (FDM) have been extensively used to analyze the behavior of such structures. FEA is a powerful

---

numerical tool that is widely utilized in structural engineering to investigate the behavior of structures subjected to various loading conditions [1]. The MDOF frames are a type of structural system that is commonly employed in modern buildings and bridges. In the MDOF frames, each floor has multiple degrees of freedom (DOF), including translational and rotational DOF [2]. The finite element method (FEM) is one of the numerical approaches that may be applied to solve engineering issues, whether they are basic or complex [3].

FEM has remained so firmly developed over the years that it now seems to be among the finest ways for examining the efficiency of a broad range of real-life situations. In fact, the approach has become one of applied mathematicians' primary research interests. The basic principle behind the finite element approach is to solve a complex issue by replacing it with a simplified solution [4]. Recently, piecewise continuous functions constructed over triangular areas have been used in the finite element approach. Researchers first proposed a lattice analogy for stress analysis in early 1906, but elastic bars with regular patterns eventually took their place [5]. The parameters of the bar were selected so that the joint's deflections could be utilized to estimate the deformations of the points in the continuum. The approach aimed to benefit from established structural analysis techniques. Most of the foregoing works presented several formulas and intricate algebraic solution methods for the first time due to a lack of available computers to develop and resolve large sets of simultaneous arithmetic problems [6]. The FEM research actually coincided with significant developments in digital computers and programming languages. Mathematicians and engineers have typically handled the hunt for different strategies to discretize continuum mechanics issues using several analytical approaches [7]. The generic techniques that may be employed to solve the governing system of differential equations were developed by mathematicians. The straightforward method and techniques for figuring out the extreme value for a function are FDM and residual methods, respectively [8].

FEM is a mathematical technique for analyzing different engineering challenges. The approach is broadly used in the analysis of solids and structures, as well as heat transport and fluids, and is fundamentally applicable in almost all domains of engineering study [9]. In engineering design and evaluation, physical issues are resolved using FEM. The framework or structural element exposed to particular external loading conditions was usually the source of the physical issues [8]. Certain assumptions are necessary for the mathematical model to idealize the physical situation, which results in differential equations guiding the model [10]. The mathematical model has a rough solution provided by FEA. The correctness of the answer must be evaluated since FEM is a numerical approach. In order to get a suitable precision, the numerical solution must be performed with improved solution parameters such as a finer mesh [11]. The analysis, which is often laborious and exceedingly thorough, must be done to get insight into the real physical issue. The choice of an approximate mathematical model is essential and entirely influences this. This necessitated the introduction of FEM in some computer-based software such as Python, MATLAB, and other computational tools to aid in accuracy assurance in the FEM analysis [12].

Due to the regrettable land shortage brought on by the fast urban population expansion in both emerging and industrialized nations, framed buildings are now the material of choice for residential and commercial constructions [13]. Structures with a combination of a slab, column, and beam can withstand lateral and gravitational stresses. These structures are often utilized to counteract the significant moments that are resulted from applied loads. The total DOF in structural frames depend on the number of nodes, and DOF is three times the number of nodes since each node has three DOF [14, 15]. When it comes to analyzing a frame under applied loads, solving it analytically can be tedious and time-consuming, especially when the frame structure possesses a large number of DOF [16]. In this research study, the matrix stiffness method of FEM for beam-column elements would be adapted and synthesized in MATLAB computational software to analyze the reactions and deformation of MDOF frames under defined loading patterns and finally validate the calculated results using results of the finite element software SAP2000 [17, 18]. The great strength of the finite-element model is its versatility since there is virtually no limit to the type of structure that can be analyzed; it provides an efficient method of static and dynamic performance assessments of structures by saving time and ensuring that economy and safety conditions are met [19].

Various studies have been done on the behavior of MDOF frames subjected to different types of loads. The use of FEA has become a popular tool to simulate and analyze the behavior of structures. In recent years, FEA has been increasingly utilized to study the behavior of MDOF frames. For instance, Li et al. [20] conducted FEA simulations using the ABAQUS software to evaluate the structural response of an eight-story reinforced concrete frame subjected to column loss scenarios. The study focused on evaluating the effectiveness of several strengthening measures, including external steel braces, reinforced concrete braces, and steel fiber-reinforced polymer sheets, in enhancing the progressive collapse resistance of the reinforced concrete frame structure.

Gao [21] performed a study to assess the seismic behavior of multi-story steel frames using FEA. They found that the use of MDOF frames can remarkably reduce the deformation and damage to the frames under seismic loads. Also,

Zhou et al. [22] utilized FEA to investigate the seismic performance of a high-rise steel building with MDOF frames. The study revealed that the MDOF frames can improve the structural stiffness and reduce the overall displacement of the building under seismic loads. In another study, Panahi et al. [23] applied FEA to examine the effect of the number of stories and the height-to-width ratio on the dynamic behavior of steel MDOF frames. The study found that increasing the number of stories and the height-to-width ratio can increase the fundamental frequency and reduce the maximum displacement of the frames. Overall, these studies suggest that FEA can be a useful tool for investigating the behavior of MDOF frames and optimizing their design parameters to improve their seismic performance. Moreover, FEA was used by Fujii [24] to analyze the behavior of a MDOF frame under earthquake loading. The results showed that the MDOF frame exhibited good resistance to earthquake loads. Similarly, in the study by Liew [25], FEA was utilized to evaluate the dynamic behavior of a multi-story MDOF frame under blast loads. The results indicated that the blast loads caused significant damage to the frame. In addition, Khalid and Bansal [26] studied the effect of the number of stories on the behavior of MDOF frames under wind loads. The results demonstrated that increasing the number of stories had a considerable effect on the behavior of the MDOF frames under wind loads.

Some potential gaps in the literature on FEA of internal forces and parametric studies of MDOF frames may include:

- Lack of studies considering the effect of uncertainties in material properties and loads on the internal forces of MDOF frames.

- Limited research on the effect of different boundary conditions on the internal forces of MDOF frames.

- Scarcity of studies on the optimization of MDOF frames based on the internal forces analysis.

- Lack of investigations that compare the accuracy and efficiency of different FEMs for the internal forces analysis of MDOF frames.

To fill these gaps, the proposed approach is to conduct a comprehensive numerical analysis and parametric study on MDOF frames using FEA. This study evaluates the effects of multiple parameters, including load type, frame geometry, and material properties. The results of the study will contribute to the development of design guidelines for MDOF frames that can be utilized in practical applications.

2. Research Methodology

The matrix stiffness displacement method, which is the indeterminate analysis method, was adopted in this study. This method is used to analyze the static and dynamic behavior of structural systems; it mainly involves expressing the equilibrium equations of a structure in terms of the displacements of its nodes [27]. The governing equations are then solved using matrix algebra, resulting in a system of simultaneous linear equations that can be solved to determine the unknown nodal displacements. The matrix stiffness displacement method is often used in FEA, where the structure is divided into smaller elements that can be modeled using simpler equations. Each element is represented by a set of stiffness and mass matrices, which are then assembled into a global stiffness and mass matrix for the entire structure [28]. The nodal displacements can be obtained by solving the resulting system of equations, and this method can handle complex geometries and boundary conditions to predict the response of a structure under varying loading conditions [29]. Results obtained in terms of internal forces were further assessed and validated using MATLAB and SAP2000 software. Additionally, the ANOVA statistical evaluation method was used to ascertain the accuracy of the computed results by testing for statistical significance at the 95% confidence interval. In order to achieve the application of this analysis method through parametric studies, the set and sequence of steps taken in this numerical analysis are presented in the flowchart shown in Figure 1.

2.1. Development of Mathematical Model

In this research, the analysis of statically indeterminate structures, frames (beam-column), was done using a finite element stiffness matrix approach to analyze the member reactions (bending moments and shear and axial forces). The beam element has four DOF, which consist of two vertical displacements and two rotations. The truss element has two axial displacements and two DOF [30–35]. If we combine these two elements, we obtain a beam-column element with six DOF, as depicted in Figure 2. Therefore, we need to formulate the stiffness matrix of a beam-column element and demonstrate how it can be used to analyze frame structures.
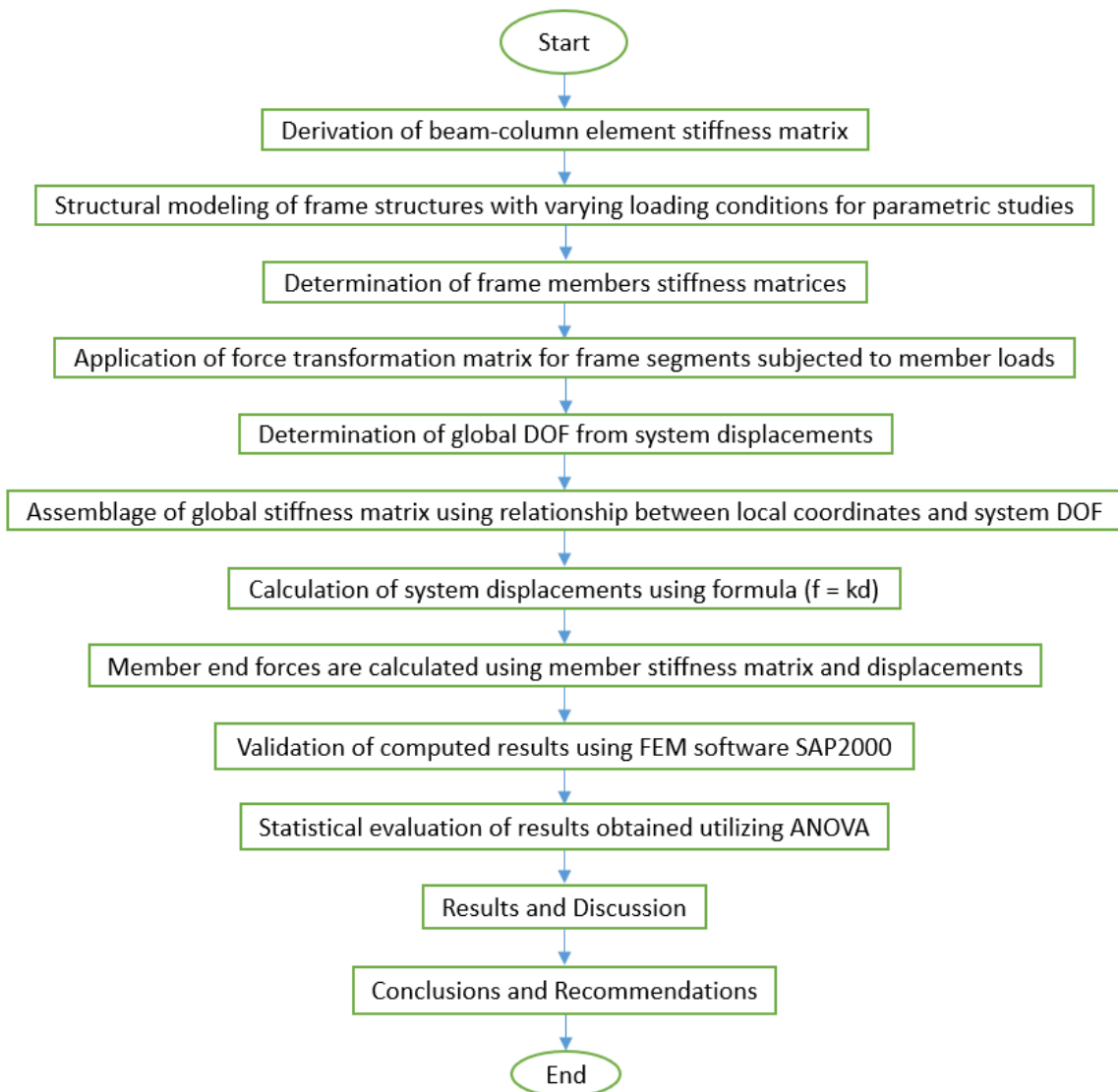
Start

Derivation of beam-column element stiffness matrix

Structural modeling of frame structures with varying loading conditions for parametric studies

Determination of frame members stiffness matrices

Application of force transformation matrix for frame segments subjected to member loads

Determination of global DOF from system displacements

Assemblage of global stiffness matrix using relationship between local coordinates and system DOF

Calculation of system displacements using formula (f = kd)

Member end forces are calculated using member stiffness matrix and displacements

Validation of computed results using FEM software SAP2000

Statistical evaluation of results obtained utilizing ANOVA

Results and Discussion

Conclusions and Recommendations

End
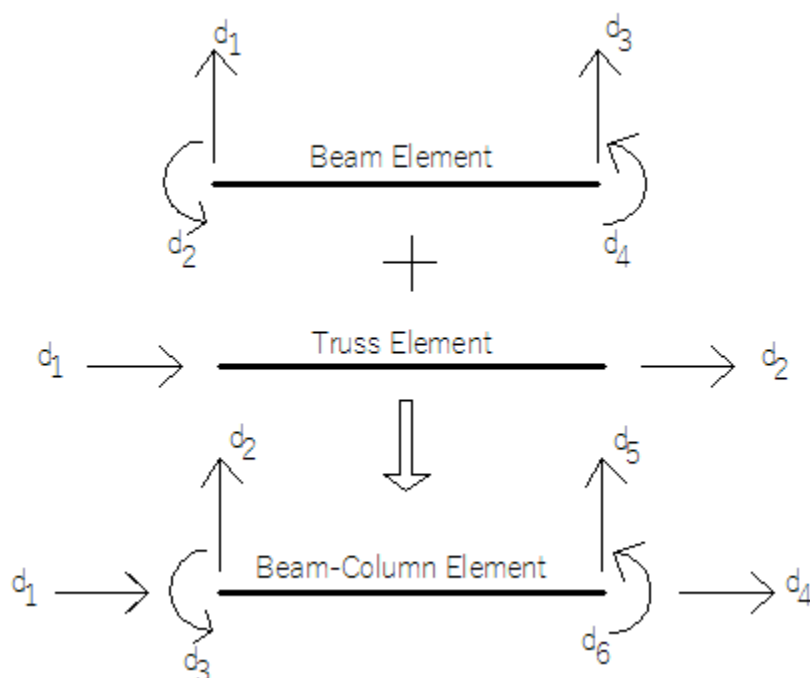
Figure 1. Flowchart of research methodology

Figure 2. Beam-column element

Given that this beam-column element has six DOF, we can define six-member end forces (f_i, for $i = 1, 2, \ldots, 6$) in the direction of the nodal displacements, as illustrated in Figure 3.
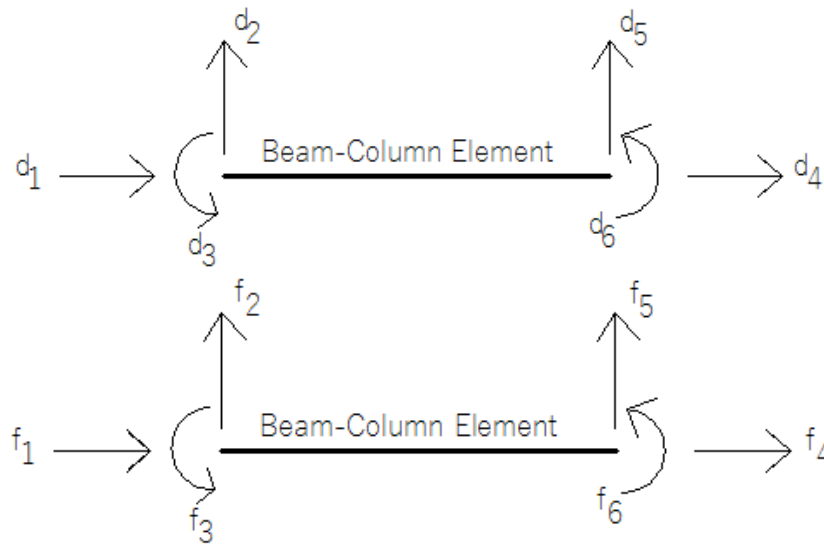

Figure 3. DOF of beam-column element

The force and displacement vectors are related to the member stiffness matrix (k) in the local coordinate system, as given in Equation 1, where f is the member force vector, k is the stiffness matrix, and d is the displacement vector. The elements of the stiffness matrix can be defined by the superposition of the beam and truss members stiffness matrices.

$$f = k_d = \begin{bmatrix} f_1 \\ f_2 \\ f_3 \\ f_4 \\ f_5 \\ f_6 \end{bmatrix} = \begin{bmatrix} k_{11} & k_{12} & k_{13} & k_{14} & k_{15} & k_{16} \\ k_{21} & k_{22} & k_{23} & k_{24} & k_{25} & k_{26} \\ k_{31} & k_{32} & k_{33} & k_{34} & k_{35} & k_{36} \\ k_{41} & k_{42} & k_{43} & k_{44} & k_{45} & k_{46} \\ k_{51} & k_{52} & k_{53} & k_{54} & k_{55} & k_{56} \\ k_{61} & k_{62} & k_{63} & k_{64} & k_{65} & k_{66} \end{bmatrix} \times \begin{bmatrix} d_1 \\ d_2 \\ d_3 \\ d_4 \\ d_5 \\ d_6 \end{bmatrix} \tag{1}$$

Figure 4 presents four DOF of the beam element, and its 4×4-member stiffness matrix size is provided in Equation 2. The matrix equation is further transformed into a 6×6 matrix because the beam-column element that we wish to define has 6 DOF (Equation 3). To achieve that, taking the numbering configuration of the element nodes into consideration, we add two rows and two columns of zeros to the matrix (k_B), as displayed in Figure 5.
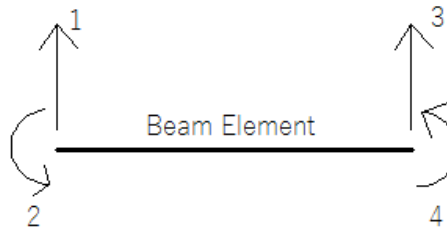

Figure 4. Four DOF of beam element

$$\begin{bmatrix} \frac{12EI}{L^3} & \frac{6EI}{L^2} & -\frac{12EI}{L^3} & \frac{6EI}{L^2} \\ \frac{6EI}{L^2} & \frac{4EI}{L} & -\frac{6EI}{L^2} & \frac{2EI}{L} \\ -\frac{12EI}{L^3} & -\frac{6EI}{L^2} & \frac{12EI}{L^3} & -\frac{6EI}{L^2} \\ \frac{6EI}{L^2} & \frac{2EI}{L} & -\frac{6EI}{L^2} & \frac{4EI}{L} \end{bmatrix} \tag{2}$$

$$k_B = \begin{bmatrix} 0 & 0 & 0 & 0 & 0 & 0 \\ 0 & \frac{12EI}{L^3} & \frac{6EI}{L^2} & 0 & -\frac{12EI}{L^3} & \frac{6EI}{L^2} \\ 0 & \frac{6EI}{L^2} & \frac{4EI}{L} & 0 & -\frac{6EI}{L^2} & \frac{2EI}{L} \\ 0 & 0 & 0 & 0 & 0 & 0 \\ 0 & -\frac{12EI}{L^3} & -\frac{6EI}{L^2} & 0 & \frac{12EI}{L^3} & -\frac{6EI}{L^2} \\ 0 & \frac{6EI}{L^2} & \frac{2EI}{L} & 0 & -\frac{6EI}{L^2} & \frac{4EI}{L} \end{bmatrix} \tag{3}$$
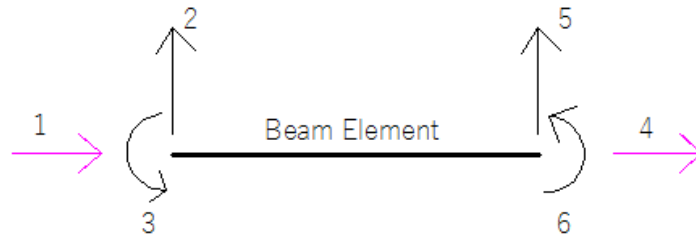
Figure 5. Expansion of beam element to obtain 6 DOF of beam-column element

In addition, Figure 6 shows two DOF of the truss element, which possesses 2×2-member stiffness matrix size, as displayed in Equation 4. The member stiffness matrix in Equation 5 is turned into a 6×6 matrix taken the numbering configuration of the element nodes into account by adding four rows and four columns of zeros (k_T), as demonstrated in Figure 7.
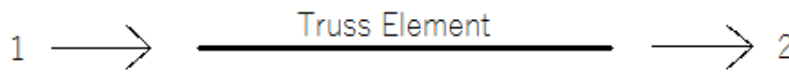

Figure 6. Two DOF of truss element

$$\begin{bmatrix} \frac{EA}{L} & -\frac{EA}{L} \\ -\frac{EA}{L} & \frac{EA}{L} \end{bmatrix} \tag{4}$$

$$k_T = \begin{bmatrix} \frac{EA}{L} & 0 & 0 & -\frac{EA}{L} & 0 & 0 \\ 0 & 0 & 0 & 0 & 0 & 0 \\ 0 & 0 & 0 & 0 & 0 & 0 \\ -\frac{EA}{L} & 0 & 0 & \frac{EA}{L} & 0 & 0 \\ 0 & 0 & 0 & 0 & 0 & 0 \\ 0 & 0 & 0 & 0 & 0 & 0 \end{bmatrix} \tag{5}$$
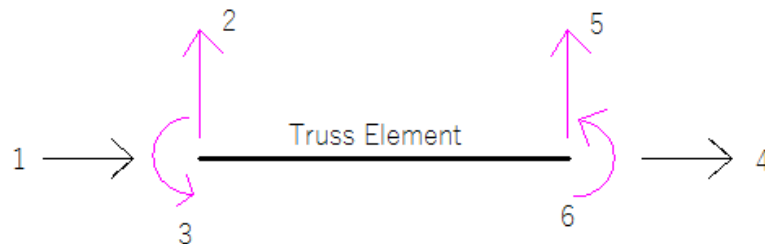

Figure 7. Expansion of truss element to obtain 6 DOF of beam-column element

When we add or superpose the developed matrices of k_T and k_B in Equation 6, we obtain the member stiffness matrix for a beam-column element, as depicted in Figure 8.

$$k = k_B + k_T = \begin{bmatrix} \frac{EA}{L} & 0 & 0 & -\frac{EA}{L} & 0 & 0 \\ 0 & \frac{12EI}{L^3} & \frac{6EI}{L^2} & 0 & -\frac{12EI}{L^3} & \frac{6EI}{L^2} \\ 0 & \frac{6EI}{L^2} & \frac{4EI}{L} & 0 & -\frac{6EI}{L^2} & \frac{2EI}{L} \\ -\frac{EA}{L} & 0 & 0 & \frac{EA}{L} & 0 & 0 \\ 0 & -\frac{12EI}{L^3} & -\frac{6EI}{L^2} & 0 & \frac{12EI}{L^3} & -\frac{6EI}{L^2} \\ 0 & \frac{6EI}{L^2} & \frac{2EI}{L} & 0 & -\frac{6EI}{L^2} & \frac{4EI}{L} \end{bmatrix} \tag{6}$$
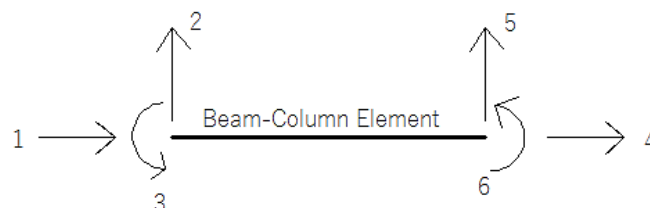

Figure 8. Six DOF of beam-column element in local coordinate system

Denoting the matrix stiffness, *k*, we can express the relationship between the member displacement and force vectors of the beam-column element in a matrix form (Equation 7). But before we can use the *k* matrix to analyze the system stiffness matrix in a structural analysis problem as the beam-column element's free body diagrams are presented in Figure 9, the derived stiffness matrix needs to transform it from the local to global system coordinates.

$$f = kd = \begin{bmatrix} f_1 \\ f_2 \\ f_3 \\ f_4 \\ f_5 \\ f_6 \end{bmatrix} = \begin{bmatrix} \frac{EA}{L} & 0 & 0 & -\frac{EA}{L} & 0 & 0 \\ 0 & \frac{12EI}{L^3} & \frac{6EI}{L^2} & 0 & -\frac{12EI}{L^3} & \frac{6EI}{L^2} \\ 0 & \frac{6EI}{L^2} & \frac{4EI}{L} & 0 & -\frac{6EI}{L^2} & \frac{2EI}{L} \\ -\frac{EA}{L} & 0 & 0 & \frac{EA}{L} & 0 & 0 \\ 0 & -\frac{12EI}{L^3} & -\frac{6EI}{L^2} & 0 & \frac{12EI}{L^3} & -\frac{6EI}{L^2} \\ 0 & \frac{6EI}{L^2} & \frac{2EI}{L} & 0 & -\frac{6EI}{L^2} & \frac{4EI}{L} \end{bmatrix} \begin{bmatrix} d_1 \\ d_2 \\ d_3 \\ d_4 \\ d_5 \\ d_6 \end{bmatrix} \quad (7)$$
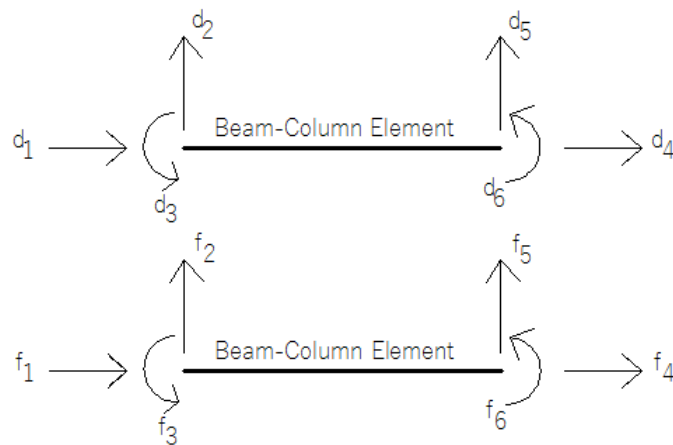

Figure 9. Force-displacement relationship

The beam-column element nodal displacement in the local coordinate system for the sake of the local-global transformation computation is illustrated in Figure 10. It is thus rotated by the angle *θ* and situated at the global coordinate system, as displayed in Figure 11.
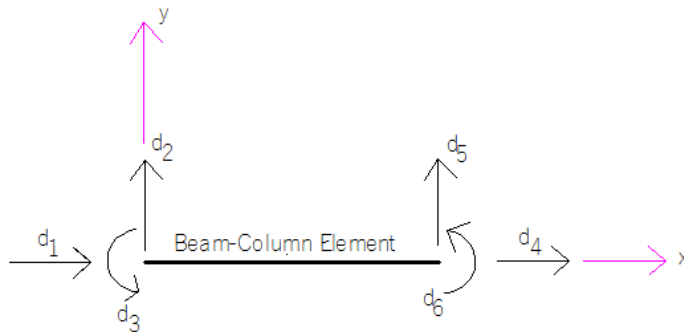

Figure 10. Displacements of beam-column element in local coordinate system
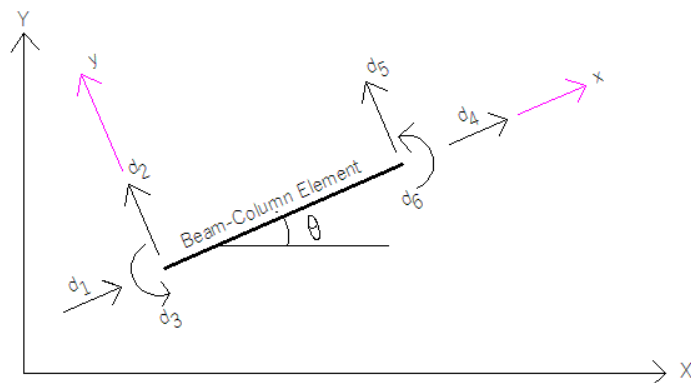

Figure 11. Local displacements of beam-column element in global coordinate system

The displacements for the beam-column element in the global coordinate system following similar rotational orientation at the angle θ can be seen in Figure 12, where the six displacements are represented as D_i for the global coordinate system [36].
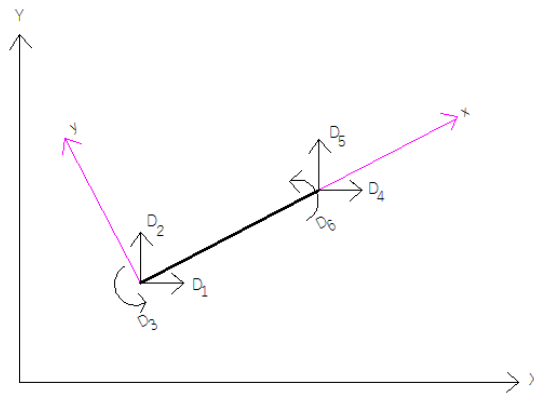

Figure 12. Global displacement in global coordinate system

We have to express each displacement in the local coordinate system, d_i, in terms of the displacements in the global coordinate system, D_i, as indicated in Figure 13.
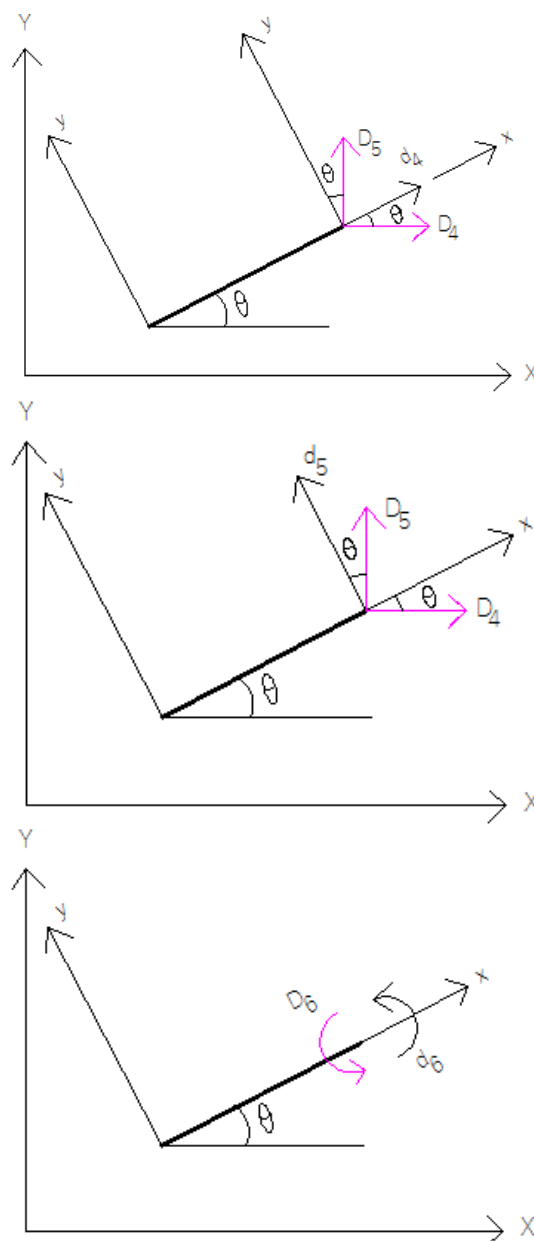

Figure 13. Diagram showing derivation of displacement transformation matrix

d_4 can be defined in terms of the global D_5 and D_4, the sum of the projection of the global displacements unto the local x-axis which is expressed mathematically in Equation 8.

$$d_4 = D_4 \cos \theta + D_5 \sin \theta \tag{8}$$

Similarly, d_5 in the local system can be considered in terms of D_4 and D_5 in the global system, as stated in Equation 9, however, d_6 is the same as the global D_6 because they both represent the rotation about the z-axis, as presented in Equation 10 [37].

$$d_5 = -D_4 \sin \theta + D_5 \cos \theta \tag{9}$$

$$d_6 = D_6 \tag{10}$$

It is worth mentioning that the rotation of the x-y plane by the angle θ does not change the orientation of the z-axis, it remains perpendicular to that plane. θ is the end rotations; converting into the matrix notation we obtain. Following the condition of symmetry, d_1, d_2, and d_3 can be written mathematically in Equations 11–13 which give us a total of six equations and denoting them in the matrix notation as presented in Equation 14 to obtain the displacement transformation matrix (T) [38].

$$d_1 = D_1 \cos \theta + D_2 \sin \theta \tag{11}$$

$$d_2 = -D_1 \sin \theta + D_2 \cos \theta \tag{12}$$

$$d_3 = D_3 \tag{13}$$

$$d = TD = \begin{bmatrix} d_1 \\ d_2 \\ d_3 \\ d_4 \\ d_5 \\ d_6 \end{bmatrix} = \begin{bmatrix} \cos \theta & \sin \theta & 0 & 0 & 0 & 0 \\ -\sin \theta & \cos \theta & 0 & 0 & 0 & 0 \\ 0 & 0 & 1 & 0 & 0 & 0 \\ 0 & 0 & 0 & \cos \theta & \sin \theta & 0 \\ 0 & 0 & 0 & -\sin \theta & \cos \theta & 0 \\ 0 & 0 & 0 & 0 & 0 & 1 \end{bmatrix} \times \begin{bmatrix} D_1 \\ D_2 \\ D_3 \\ D_4 \\ D_5 \\ D_6 \end{bmatrix} \tag{14}$$

We can also achieve a similar matrix for the force transformation matrix (Q) by presenting the nodal forces for the beam-column element rotated through the angle θ. The member forces in the local (f_i) and global coordinate system (F_i) are demonstrated in Figure 14 [39].
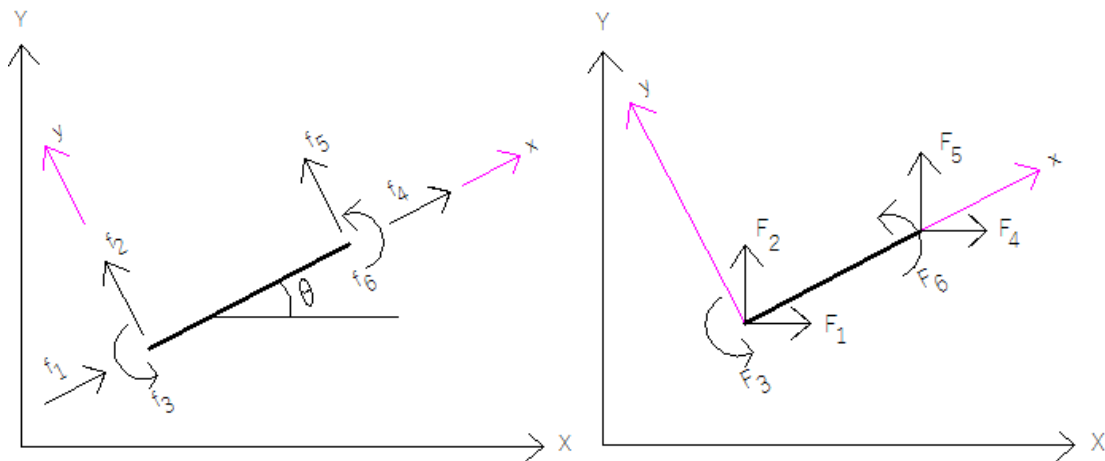
Figure 14. Local forces and global forces in global coordinate system

Now, we define the global F_4 in terms of the local forces f_4 and f_5, which can be achieved by adding the projection of the local f_4 and f_5 unto the global F_4 axis (Equation 15).

$$F_4 = f_4 \cos \theta - f_5 \sin \theta \tag{15}$$

Similarly, F_5 can be represented mathematically, in terms of the end rotation θ and the local forces f_4 and f_5 in Equation 16. F_6 is the same as the local force f_6, as given in Equation 17 [40].

$$F_5 = f_4 \sin \theta + f_5 \cos \theta \tag{16}$$

$$F_6 = f_6 \tag{17}$$

The graphical expression of the six local forces f_i in terms of the forces in the global coordinate system F_i is indicated in Figure 15. Following the condition of symmetry, the global forces F_1, F_2, and F_3 can be written mathematically (Equations 18–20). These six sets of equations can be provided in the matrix form as in Equation 21 to obtain the force transformation matrix (Q) [41].

$$F_1 = f_1 \cos \theta - f_2 \sin \theta \tag{18}$$

$$F_2 = f_1 \sin \theta + f_2 \cos \theta \tag{19}$$

$$F_3 = f_3 \tag{20}$$

$$F = Qf = \begin{bmatrix} F_1 \\ F_2 \\ F_3 \\ F_4 \\ F_5 \\ F_6 \end{bmatrix} = \begin{bmatrix} \cos \theta & -\sin \theta & 0 & 0 & 0 & 0 \\ \sin \theta & \cos \theta & 0 & 0 & 0 & 0 \\ 0 & 0 & 1 & 0 & 0 & 0 \\ 0 & 0 & 0 & \cos \theta & -\sin \theta & 0 \\ 0 & 0 & 0 & \sin \theta & \cos \theta & 0 \\ 0 & 0 & 0 & 0 & 0 & 1 \end{bmatrix} \times \begin{bmatrix} f_1 \\ f_2 \\ f_3 \\ f_4 \\ f_5 \\ f_6 \end{bmatrix} \tag{21}$$
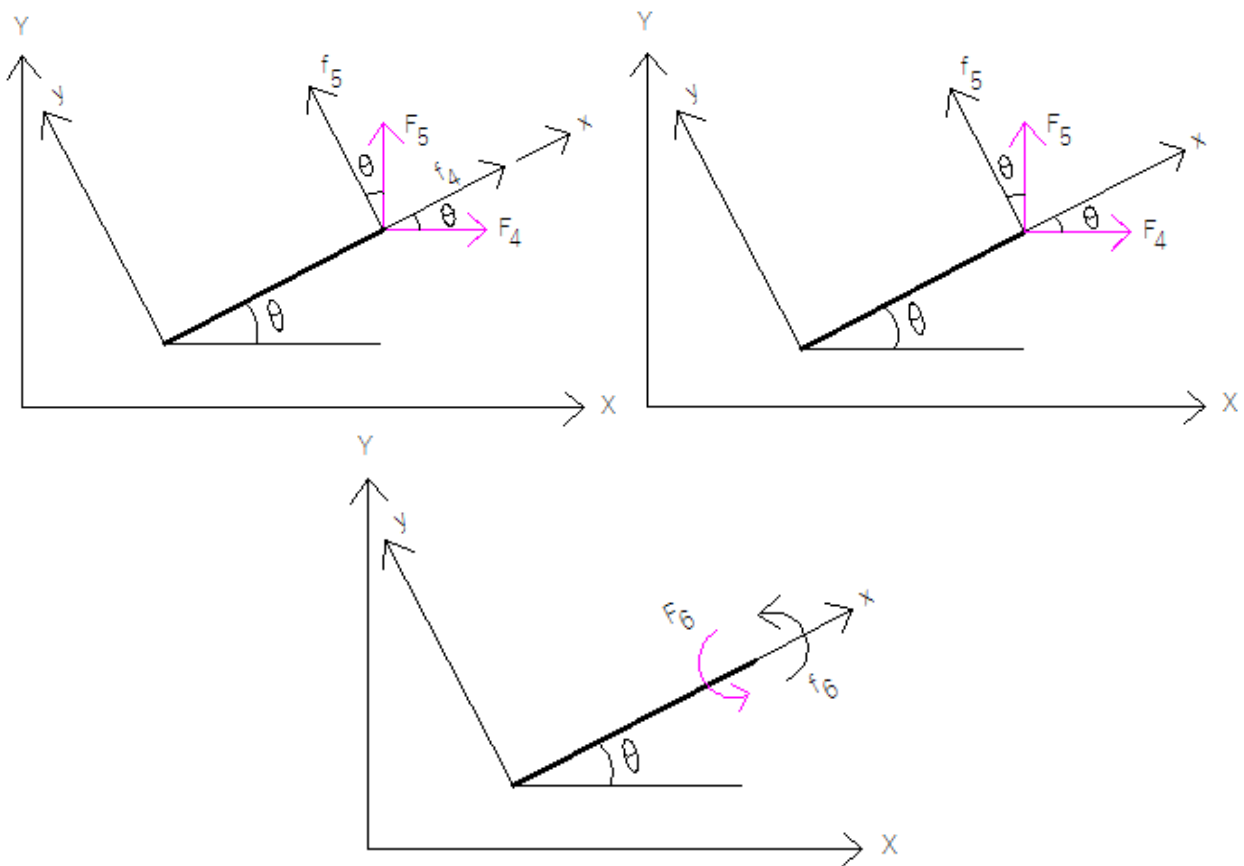

Figure 15. Diagram showing derivation of force transformation matrix

With these mathematical derivations and transformation matrices, we can then obtain the stiffness matrix at the global coordinate system, which starts by writing the stiffness matrix in the local coordinate system for the force displacement relationship, as depicted in Figure 9. This expression is provided in Equation 22, and by multiplying the equation by the force transformation matrix (Q) on both sides of the equation, we get Equation 23. However, recalling the force transformation (Q) relationship, we can observe that $F = Q_f$ and is substituted into Equation 21 to obtain the relationship with the forces at the global coordinates (F_i) in Equation 24 [42, 43].

$$f = k \times d \tag{22}$$

$$Q \times f = Q \times k \times d \tag{23}$$

$$F = Q \times k \times d \tag{24}$$

Also, by considering the displacement transformation matrix (T) relationship which implies that $d = TD$ and substituting the expression into Equation 24, we can obtain a generalized mathematical relationship as Equation 25.

$$F = Q \times k \times T \times D \tag{25}$$

The three principal parameters taken for the derivation of Equation 25 are the force transformation matrix, member stiffness matrix in the local coordinate, and the displacement transformation matrix, as presented in Equations 21, 7, and 14, respectively. By multiplying Q, k, and T matrices, we obtain the expression for the global stiffness matrix of the beam-column element, as given in Equation 26. This is used to assemble system stiffness matrices when analyzing indeterminate frame structures [44].

$$K = QkT = \begin{bmatrix} 12\beta s^2 + \alpha c^2 & -12\beta cs + \alpha cs & -6\beta Ls & -12\beta s^2 - \alpha c^2 & 12\beta cs - \alpha cs & -6\beta Ls \\ -12\beta cs + \alpha cs & 12\beta c^2 + \alpha c^2 & 6\beta Lc & 12\beta cs - \alpha cs & -12\beta c^2 - \alpha s^2 & 6\beta Lc \\ -6\beta Ls & 6\beta Lc & 4\beta L^2 & 6\beta Ls & -6\beta Lc & 2\beta L^2 \\ -12\beta s^2 - \alpha c^2 & 12\beta cs - \alpha cs & 6\beta Ls & 12\beta s^2 + \alpha s^2 & -12\beta cs + \alpha cs & 6\beta Ls \\ 12\beta cs - \alpha cs & -12\beta c^2 - \alpha s^2 & -6\beta Lc & -12\beta cs + \alpha c & 12\beta c^2 + \alpha s^2 & -6\beta Lc \\ -6\beta Ls & 6\beta Lc & 2\beta L^2 & 6\beta Ls & -6\beta Lc & 4\beta L^2 \end{bmatrix} \tag{26}$$

where $\alpha = \frac{EA}{L}$; $\beta = \frac{EI}{L^3}$; $c = \cos\theta$; $s = \sin\theta$; E is the modulus of elasticity; A is the cross-sectional area; I is the moment of inertia about the axis of bending.

2.2. Structural Modeling of MDOF Frame for Parametric Studies

The following nine steps are taken in the beam-column finite element application for the analysis of indeterminate frame structures [45].

1. Apply the member stiffness matrix formula and determine the member stiffness matrices without load effects.

2. Analyze the applied loads to obtain the member fixed end forces.

3. Apply the force transformation matrix computation for cases with member loads.

4. Determine DOF of the frame at the global coordinate by analyzing the imposed support conditions.

5. Associate DOF for the members (local coordinate) with the derived DOF at the global coordinate.

6. Assemble the global stiffness matrix using the relationship derived in the step 5 above.

7. Derive the system displacements (global coordinate) using Equation 22 i.e., relationship between the global stiffness matrix, displacement, and fixed end forces.

8. Transform the calculated system displacements into local coordinate systems.

9. Determine the member forces (bending moments and shear and axial forces) with the aid of derived member displacements, calculated member stiffness, and applied member forces.

Formulation of frame structures were first taken for the study which are loaded on the distinct points namely, member and joint loads. The indeterminate frame for this study is illustrated in Figures 16 and 17 with the constant modulus of elasticity (E), moment of Inertia (I), and cross-sectional area (A) of 200 GPa, $30{\times}10^6$ mm^4, and 5000 mm^2, respectively.
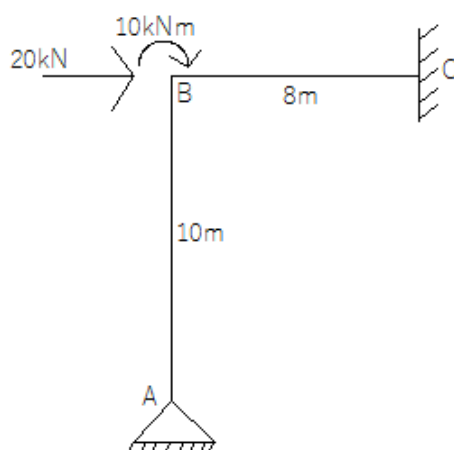

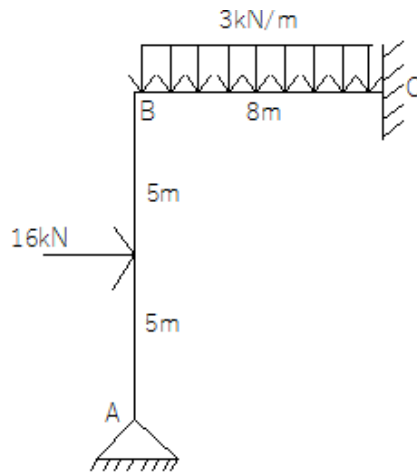**Figure 16. Parametric study, Case 1**

Figure 17. Parametric study, Case 2

Without joint loads, the member equations can be expressed as in Equation 22 where f is the force vector, d is the displacement vector, and k is the stiffness matrix. However, when the member is subjected to a load either concentrated or distributed, then the equation is transformed to Equation 27 where p represents fixed end forces due to the member loads. In the cases of uniformly distributed load w applied to a member with the length l, concentrated load p applied to the center of the member with the length l, and concentrated load p applied at arbitrary points between a and b of the member length l, the elements of p for the three load patterns are displayed in Equation 28 specified in the member's local coordinate system. When transformed to the global coordinate system, Equation 27 is transformed to Equation 29 where Q is the force transformation matrix. Assuming that, $P = Qp$, where P is the vector of fixed end forces specified in the global coordinate system which is used to determine the system joint loads [46, 47].

$$f = (k \times d) + p \tag{27}$$

$$p = \begin{Bmatrix} 0 \\ \frac{wl}{2} \\ \frac{wl^2}{12} \\ 0 \\ \frac{wl}{2} \\ -\frac{wl^2}{12} \end{Bmatrix} \qquad p = \begin{Bmatrix} 0 \\ \frac{p}{2} \\ \frac{pl}{8} \\ 0 \\ \frac{p}{2} \\ -\frac{pl}{8} \end{Bmatrix} \qquad p = \begin{Bmatrix} 0 \\ \frac{pb}{l} \\ \frac{pab^2}{l^2} \\ 0 \\ \frac{pa}{l} \\ -\frac{pa^2b}{l^2} \end{Bmatrix} \tag{28}$$

$$F = (K \times D) + (Q \times p) \tag{29}$$

In line with the forgoing, one-story frame with concentrated member loads was modeled for the analysis (Figure 18) with the constant modulus of elasticity (E) of 200 GPa and moment of inertia (I) and cross-sectional area (A) of 640×10^6 mm^4 and 11700 mm^2, respectively for the horizontal member (BC), and moment of inertia (I) and cross-sectional area (A) of 330×10^6 mm^4 and 9500 mm^2, respectively for the vertical members (AB and CD).
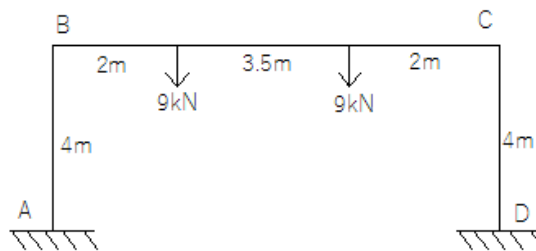
Figure 18. Parametric study, Case 3

The reactions (bending moments and shear and axial forces) are calculated from the statically indeterminate frame and are statistically compared with analytical solutions obtained from SAP2000 software using student's t-test. The MATAB and Microsoft Excel software are adapted for the matrix computation and analysis to derive accurate result [48, 49].

3. Analysis and Iterative Solutions

The developed beam-column element stiffness matrix was deployed for the analysis of indeterminate frame structures to derive the reactions (bending moments and shear and axial forces) due to applied joint and member loads. The formulated element stiffness matrix formula was synthesized in the MATLAB software and the solutions for the three cases investigated for the parametric assessments are presented according to the stated steps as follows [50].

3.1. Case 1: L-Shaped Frame Supported by Pin and Fixed Supports at Two Ends with Joint Load

3.1.1. Derivation of Member Stiffness Matrix

Parameters for the member AB are presented below.

$$\alpha = \frac{EA}{L} = \frac{(200000000)(0.005)}{10} = 100000; \quad \beta = \frac{EI}{L^3} = \frac{(200000000)(0.00003)}{1000} = 6$$

$$\cos(\theta) = \cos(90) = 0; \sin(\theta) = \sin(90) = 1$$

Therefore, by substituting the parameters into the member stiffness matrix formula we obtain Equation 30.

$$K_{AB} = \begin{bmatrix} 72 & 0 & -360 & -72 & 0 & -360 \\ 0 & 100000 & 0 & 0 & 100000 & 0 \\ -360 & 0 & 2400 & 360 & 0 & 1200 \\ -72 & 0 & 360 & 72 & 0 & 360 \\ 0 & 100000 & 0 & 0 & 100000 & 0 \\ -360 & 0 & 12000 & 360 & 0 & 2400 \end{bmatrix} \tag{30}$$

Parameters for the member BC are as following.

$$\alpha = \frac{EA}{L} = \frac{(200000000)(0.005)}{8} = 125000; \quad \beta = \frac{EI}{L^3} = \frac{(200000000)(0.00003)}{512} = 11.72$$

$$\cos(\theta) = \cos(0) = 1; \sin(\theta) = \sin(0) = 0$$

Equation 31 can be achieved by substituting the parameters into the member stiffness matrix formula.

$$K_{BC} = \begin{bmatrix} 125000 & 0 & 0 & -125000 & 0 & 0 \\ 0 & 140.625 & 562.5 & 0 & -140.625 & 562.5 \\ 0 & 562.5 & 3000 & 0 & -562.5 & 1500 \\ -125000 & 0 & 0 & 125000 & 0 & 0 \\ 0 & -140.625 & -562.5 & 0 & 140.625 & -562.5 \\ 0 & 562.5 & 1500 & 0 & -562.5 & 3000 \end{bmatrix} \tag{31}$$

3.1.2. Assembling of System Matrix

Since there are no member loads, there is no need for the force transformation computation and hence, the imposed joint loads are taken as the fixed end forces corresponding to the numbering orientation of the defined DOF in the global coordinate, as demonstrated in Figure 19. The three DOF for the beam-column element at the local coordinate associated with the derived four DOF at the global coordinate were added to assemble the global stiffness matrix, as presented in Equations 32 and 33 [51].
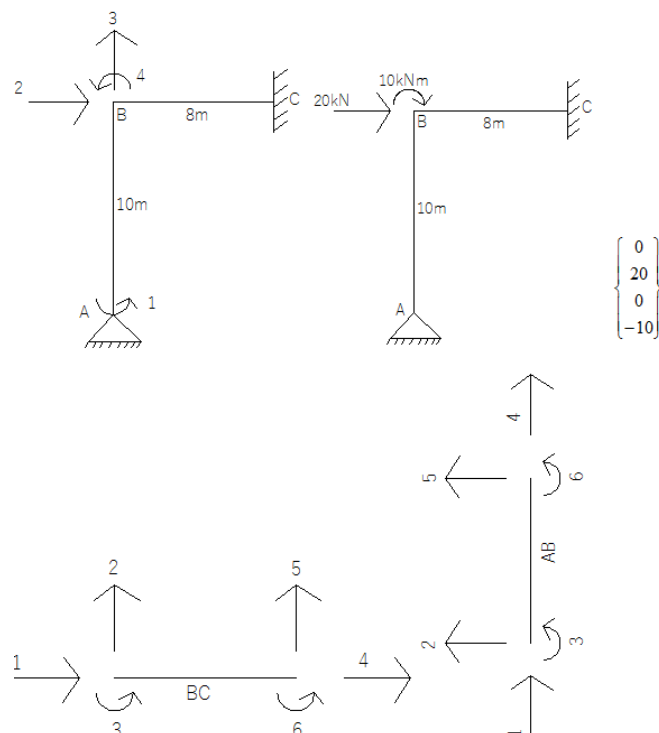

Figure 19. DOF in global coordinates and derivation of force vector from applied joint loads, Case 1

$$k_{11} = k_{33}^{AB} \quad k_{12} = k_{34}^{AB} \quad k_{13} = k_{35}^{AB} \quad k_{14} = k_{36}^{AB} \quad k_{22} = k_{44}^{AB} + k_{11}^{BC} \quad k_{23} = k_{45}^{AB} + k_{12}^{BC} \quad k_{24} = k_{46}^{AB} + k_{13}^{BC} \quad k_{33} =$$
$$k_{55}^{AB} + k_{22}^{BC} \quad k_{34} = k_{56}^{AB} + k_{23}^{BC} \quad k_{44} = k_{66}^{AB} + k_{33}^{BC}$$

(32)

$$K = \begin{bmatrix} 2400 & 360 & 0 & 1200 \\ 0 & 125072 & 0 & 360 \\ 0 & 0 & 100140.6 & 562.5 \\ 1200 & 360 & 562.5 & 5400 \end{bmatrix}$$

(33)

3.1.3. Derivation of System Displacements

Using the derived system stiffness matrix and force vector and substituting in Equation 22, the displacements in the global coordinates are obtained in Equation 34.

$$\begin{bmatrix} 2400 & 360 & 0 & 1200 \\ 0 & 125072 & 0 & 360 \\ 0 & 0 & 100140.6 & 562.5 \\ 1200 & 360 & 562.5 & 5400 \end{bmatrix} \begin{Bmatrix} D_1 \\ D_2 \\ D_3 \\ D_4 \end{Bmatrix} = \begin{Bmatrix} 0 \\ 20 \\ 0 \\ -10 \end{Bmatrix}; \quad \begin{Bmatrix} D_1 \\ D_2 \\ D_3 \\ D_4 \end{Bmatrix} = \begin{Bmatrix} 0.00102 \\ 0.000163 \\ 0.00012 \\ -0.0021 \end{Bmatrix}$$

(34)

3.1.4. Calculation of Member Forces

The computed system displacements are first transformed into the local coordinates (Figure 20), after which the derived member displacements are substituted in Equation 22 to determine the member forces, as indicated in Figure 21 and Equations 35 and 36 respectively for the members AB and BC [52].
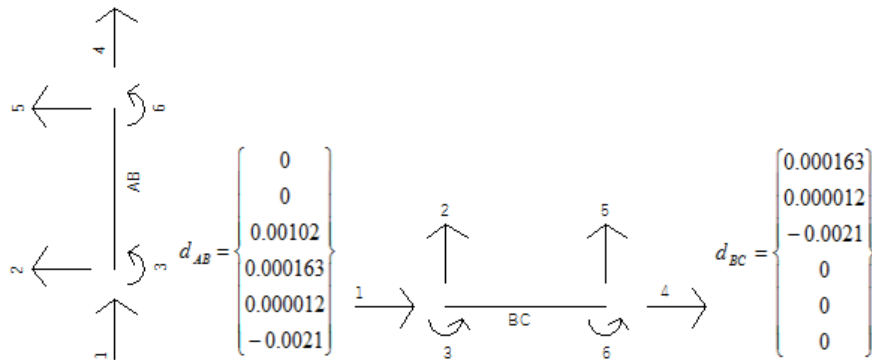
Figure 20. Transformation of system displacements to local coordinates, Case 1
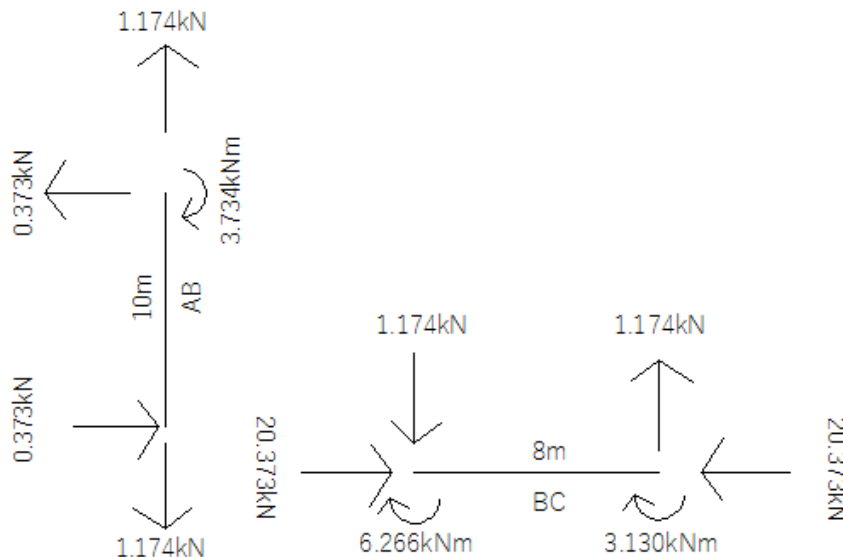
Figure 21. Member forces in free body diagram, Case 1

$$\begin{Bmatrix} f_1 \\ f_2 \\ f_3 \\ f_4 \\ f_5 \\ f_6 \end{Bmatrix} = \begin{bmatrix} 72 & 0 & -360 & -72 & 0 & -360 \\ 0 & 100000 & 0 & 0 & 100000 & 0 \\ -360 & 0 & 2400 & 360 & 0 & 1200 \\ -72 & 0 & 360 & 72 & 0 & 360 \\ 0 & 100000 & 0 & 0 & 100000 & 0 \\ -360 & 0 & 12000 & 360 & 0 & 2400 \end{bmatrix} \begin{Bmatrix} 0 \\ 0 \\ 0.00102 \\ 0.000163 \\ 0.000012 \\ -0.0021 \end{Bmatrix} = \begin{Bmatrix} 0.373 \\ -1.174 \\ 0 \\ -0.373 \\ 1.174 \\ -3.734 \end{Bmatrix}$$

(35)

$$\begin{Bmatrix} f_1 \\ f_2 \\ f_3 \\ f_4 \\ f_5 \\ f_6 \end{Bmatrix} = \begin{bmatrix} 125000 & 0 & 0 & -125000 & 0 & 0 \\ 0 & 140.625 & 562.5 & 0 & -140.625 & 562.5 \\ 0 & 562.5 & 3000 & 0 & -562.5 & 1500 \\ -125000 & 0 & 0 & 125000 & 0 & 0 \\ 0 & -140.625 & -562.5 & 0 & 140.625 & -562.5 \\ 0 & 562.5 & 1500 & 0 & -562.5 & 3000 \end{bmatrix} \begin{Bmatrix} 0.000163 \\ 0.000012 \\ -0.0021 \\ 0 \\ 0 \\ 0 \end{Bmatrix} = \begin{Bmatrix} 20.373 \\ -1.174 \\ -6.266 \\ -20.373 \\ 1.174 \\ -3.130 \end{Bmatrix} \tag{36}$$

3.2. Case 2: L-Shaped Frame Supported by Pin and Fixed Supports at Two Ends with Member Loads

3.2.1. Derivation of Member Stiffness Matrix

Since the frame has similar geometry and flexural rigidity parameters as the Case 1 frame, the member stiffness matrices are the same, as presented in Equations 30 and 31. Therefore,

$$K_{AB} = \begin{bmatrix} 72 & 0 & -360 & -72 & 0 & -360 \\ 0 & 100000 & 0 & 0 & 100000 & 0 \\ -360 & 0 & 2400 & 360 & 0 & 1200 \\ -72 & 0 & 360 & 72 & 0 & 360 \\ 0 & 100000 & 0 & 0 & 100000 & 0 \\ -360 & 0 & 12000 & 360 & 0 & 2400 \end{bmatrix}; K_{BC} = \begin{bmatrix} 125000 & 0 & 0 & -125000 & 0 & 0 \\ 0 & 140.625 & 562.5 & 0 & -140.625 & 562.5 \\ 0 & 562.5 & 3000 & 0 & -562.5 & 1500 \\ -125000 & 0 & 0 & 125000 & 0 & 0 \\ 0 & -140.625 & -562.5 & 0 & 140.625 & -562.5 \\ 0 & 562.5 & 1500 & 0 & -562.5 & 3000 \end{bmatrix}$$

3.2.2. Analysis and Transformation of Member Loads

The member loads on the frame structures are analyzed to convert them to fixed end forces using Equation 28 for the imposed concentrated and distributed loads, and by substituting the defined parameters we obtain Equation 37.

$$pAB = \begin{Bmatrix} 0 \\ 8 \\ 20 \\ 0 \\ 8 \\ -20 \end{Bmatrix}; pBC = \begin{Bmatrix} 0 \\ 12 \\ 16 \\ 0 \\ 12 \\ -16 \end{Bmatrix} \tag{37}$$

Furthermore, the derived Equation 37 is multiplied by the force transformation matrix (Q) to obtain the member fixed end forces as in Equation 38. Accordingly, the system force vector is presented in Equation 39 [53]. The calculated fixed end forces are thus displayed in a free body diagram, and based on support conditions, the reactions at the fixed supports are disregarded with the translational reaction in the pinned support, as demonstrated in Figure 22.

$$f_{AB} = \begin{Bmatrix} 0 \\ 8 \\ 20 \\ 0 \\ 8 \\ -20 \end{Bmatrix} \times \begin{bmatrix} 0 & -1 & 0 & 0 & 0 & 0 \\ 1 & 0 & 0 & 0 & 0 & 0 \\ 0 & 0 & 1 & 0 & 0 & 0 \\ 0 & 0 & 0 & 0 & -1 & 0 \\ 0 & 0 & 0 & 1 & 0 & 0 \\ 0 & 0 & 0 & 0 & 0 & 1 \end{bmatrix} = \begin{Bmatrix} -8 \\ 0 \\ 20 \\ -8 \\ 0 \\ -20 \end{Bmatrix}; f_{BC} = \begin{Bmatrix} 0 \\ 12 \\ 16 \\ 0 \\ 12 \\ -16 \end{Bmatrix} \times \begin{bmatrix} 1 & 0 & 0 & 0 & 0 & 0 \\ 0 & 1 & 0 & 0 & 0 & 0 \\ 0 & 0 & 1 & 0 & 0 & 0 \\ 0 & 0 & 0 & 1 & 0 & 0 \\ 0 & 0 & 0 & 0 & 1 & 0 \\ 0 & 0 & 0 & 0 & 0 & 1 \end{bmatrix} = \begin{Bmatrix} 0 \\ 12 \\ 16 \\ 0 \\ 12 \\ -16 \end{Bmatrix} \tag{38}$$

$$F = \begin{Bmatrix} -20 \\ 8 \\ -12 \\ 4 \end{Bmatrix} \tag{39}$$
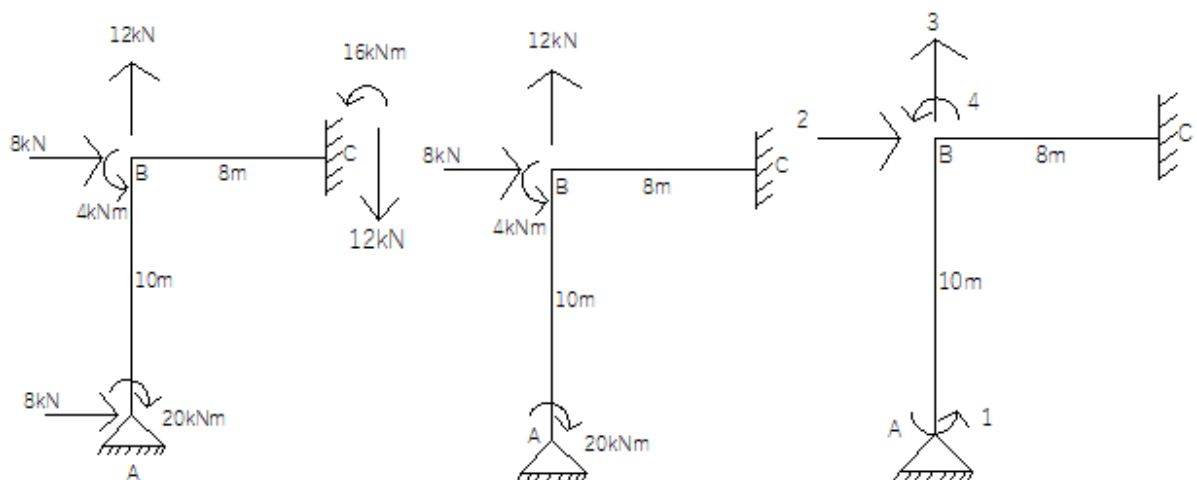

Figure 22. Free body diagrams illustrating joint reactions due to member loads, Case 2

3.2.3. Assembling of System Matrix

Similar to the assemblage of the global stiffness matrix for the Case 1 parametric study, the three DOF for the beam-column element at the local coordinate were systematically associated with the derived four DOF at the global coordinate to assemble the global stiffness matrix, as mentioned in Equation 40 [54].

$$K = \begin{bmatrix} 2400 & 360 & 0 & 1200 \\ 0 & 125072 & 0 & 360 \\ 0 & 0 & 100140.6 & 562.5 \\ 1200 & 360 & 562.5 & 5400 \end{bmatrix} \tag{40}$$

3.2.4. Derivation of System Displacements

Utilizing the derived system stiffness matrix and force vector and substituting in Equation 22, the displacements in the global coordinates are obtained in Equation 41.

$$\begin{bmatrix} 2400 & 360 & 0 & 1200 \\ 0 & 125072 & 0 & 360 \\ 0 & 0 & 100140.6 & 562.5 \\ 1200 & 360 & 562.5 & 5400 \end{bmatrix} \begin{Bmatrix} D_1 \\ D_2 \\ D_3 \\ D_4 \end{Bmatrix} = \begin{Bmatrix} -20 \\ 8 \\ -12 \\ 4 \end{Bmatrix}; \quad \begin{Bmatrix} D_1 \\ D_2 \\ D_3 \\ D_4 \end{Bmatrix} = \begin{Bmatrix} -0.00981 \\ 0.0000838 \\ -0.000136 \\ 0.00293 \end{Bmatrix} \tag{41}$$

3.2.5. Calculation of Member Forces

The computed system displacements are first transformed into the local coordinates in accordance with the numbering configuration of the frame structure at the global coordinate, as indicated in Figure 23. Furthermore, the derived member displacements are substituted in Equation 27 to determine the member forces, as depicted in Figure 24 and Equation 42 and 43 for the members AB and BC, respectively [46].
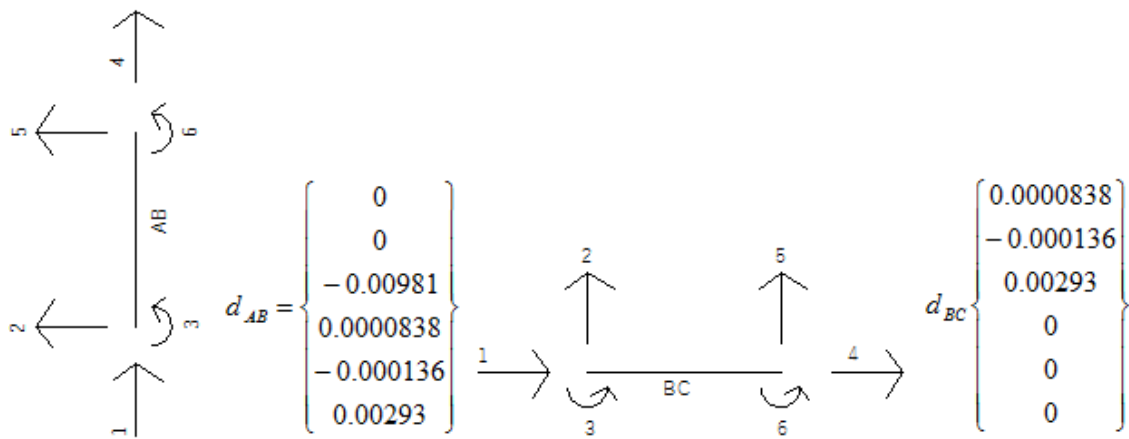

Figure 23. Transformation of system displacements to local coordinates, Case 2
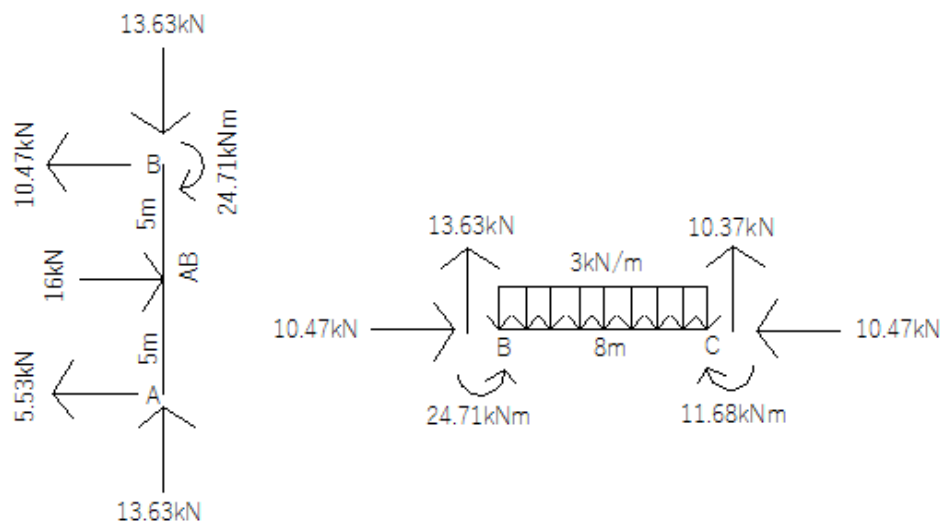

Figure 24. Member forces in free body diagram, Case 2

$$\begin{Bmatrix} f_1 \\ f_2 \\ f_3 \\ f_4 \\ f_5 \\ f_6 \end{Bmatrix} = \begin{bmatrix} 72 & 0 & -360 & -72 & 0 & -360 \\ 0 & 100000 & 0 & 0 & 100000 & 0 \\ -360 & 0 & 2400 & 360 & 0 & 1200 \\ -72 & 0 & 360 & 72 & 0 & 360 \\ 0 & 100000 & 0 & 0 & 100000 & 0 \\ -360 & 0 & 12000 & 360 & 0 & 2400 \end{bmatrix} \begin{Bmatrix} 0 \\ 0 \\ -0.00981 \\ 0.0000838 \\ -0.000136 \\ 0.00293 \end{Bmatrix} + \begin{Bmatrix} -8 \\ 0 \\ 20 \\ -8 \\ 0 \\ -20 \end{Bmatrix} = \begin{Bmatrix} -5.53 \\ 13.63 \\ 0 \\ -10.47 \\ -13.63 \\ -24.71 \end{Bmatrix} \tag{42}$$

$$\begin{Bmatrix} f_1 \\ f_2 \\ f_3 \\ f_4 \\ f_5 \\ f_6 \end{Bmatrix} = \begin{bmatrix} 125000 & 0 & 0 & -125000 & 0 & 0 \\ 0 & 140.625 & 562.5 & 0 & -140.625 & 562.5 \\ 0 & 562.5 & 3000 & 0 & -562.5 & 1500 \\ -125000 & 0 & 0 & 125000 & 0 & 0 \\ 0 & -140.625 & -562.5 & 0 & 140.625 & -562.5 \\ 0 & 562.5 & 1500 & 0 & -562.5 & 3000 \end{bmatrix} \begin{Bmatrix} 0.0000838 \\ -0.000136 \\ 0.00293 \\ 0 \\ 0 \\ 0 \end{Bmatrix} + \begin{Bmatrix} 0 \\ 12 \\ 16 \\ 0 \\ 12 \\ -16 \end{Bmatrix} = \begin{Bmatrix} 10.47 \\ 13.63 \\ 24.71 \\ -10.47 \\ 10.37 \\ -11.68 \end{Bmatrix} \tag{43}$$

3.3. Case 3: One-Story Frame Constrained by Fixed Supports and Symmetrically Loaded

3.3.1. Derivation of Member Stiffness Matrix

Parameters for the vertical members AB and DC with similar geometry and flexural rigidity are provided in the following.

$$\alpha = \frac{EA}{L} = \frac{(200000000)(0.0095)}{4} = 475000; \beta = \frac{EI}{L^3} = \frac{(200000000)(0.00033)}{4^3} = 1031.25$$

$$cos(\theta) = cos(90) = 0; sin(\theta) = sin(90) = 1$$

Consequently, Equation 44 is achieved by substituting the parameters into the member stiffness matrix formula.

$$K_{AB} = K_{DC} = \begin{bmatrix} 12375 & 0 & -24750 & -12375 & 0 & -24750 \\ 0 & 475000 & 0 & 0 & -475000 & 0 \\ -24750 & 0 & 66000 & 24750 & 0 & 33000 \\ -12375 & 0 & 24750 & 12375 & 0 & 24750 \\ 0 & -475000 & 0 & 0 & 475000 & 0 \\ -24750 & 0 & 33000 & 24750 & 0 & 66000 \end{bmatrix} \tag{44}$$

Parameters for the member BC are demonstrated below.

$$\alpha = \frac{EA}{L} = \frac{(200000000)(0.0117)}{7.5} = 31200; \beta = \frac{EI}{L^3} = \frac{(200000000)(0.00064)}{7.5^3} = 303.41$$

$$cos(\theta) = cos(0) = 1; sin(\theta) = sin(0) = 0$$

Moreover, by substituting the parameters into the member stiffness matrix formula we obtain Equation 45.

$$K_{BC} = \begin{bmatrix} 312000 & 0 & 0 & 312000 & 0 & 0 \\ 0 & 3641 & 13653 & 0 & -3641 & 13653 \\ 0 & 13653 & 68267 & 0 & -13653 & 34133 \\ 312000 & 0 & 0 & 312000 & 0 & 0 \\ 0 & -3641 & -13653 & 0 & 3641 & -13653 \\ 0 & 13653 & 34133 & 0 & -13653 & 68267 \end{bmatrix} \tag{45}$$

3.3.2. Analysis and Transformation of Member Loads

The member loads on the frame structures are analyzed to convert them to fixed end forces utilizing Equation 28 which are shown in Figure 25 for the load applied at distance a from the left end and b from the right end with the beam length (L). Due to the loading configuration in the member, the principle of superposition is deployed to calculate the fixed end forces, as depicted in Figure 26 [51].
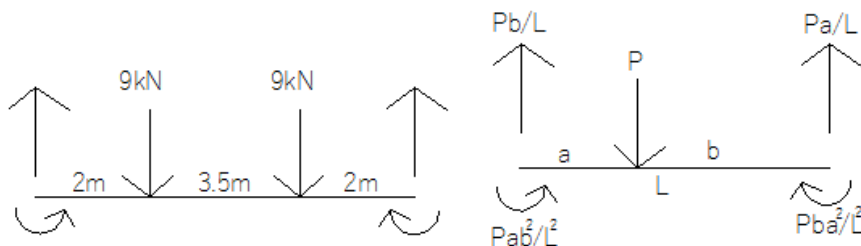

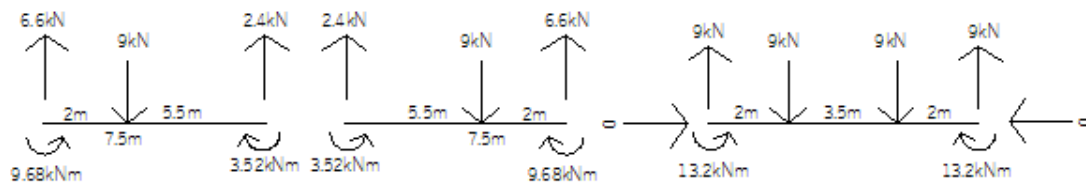**Figure 25. Fixed end forces due to applied concentrated load, Case 3**

Figure 26. Application of principle of superposition to obtain fixed end forces, Case 3

The derived fixed end forces for the member BC are given in the matrix form and multiplied by the force transformation matrix (Q), as reported in Equation 46. The free body diagram with the calculated fixed end forces is represented in Figure 27 [44, 55].

$$pBC = \begin{Bmatrix} 0 \\ -9 \\ -13.2 \\ 0 \\ -9 \\ 13.2 \end{Bmatrix} f_{BC} = \begin{Bmatrix} 0 \\ -9 \\ -13.2 \\ 0 \\ -9 \\ 13.2 \end{Bmatrix} \times \begin{bmatrix} 1 & 0 & 0 & 0 & 0 & 0 \\ 0 & 1 & 0 & 0 & 0 & 0 \\ 0 & 0 & 1 & 0 & 0 & 0 \\ 0 & 0 & 0 & 1 & 0 & 0 \\ 0 & 0 & 0 & 0 & 1 & 0 \\ 0 & 0 & 0 & 0 & 0 & 1 \end{bmatrix} = \begin{Bmatrix} 0 \\ -9 \\ -13.2 \\ 0 \\ -9 \\ 13.2 \end{Bmatrix} \tag{46}$$
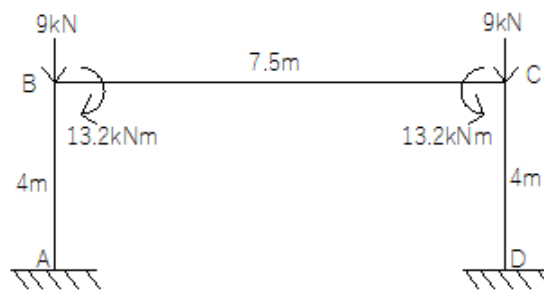
Figure 27. Free body diagram illustrating calculated fixed end forces, Case 3

3.3.3. Assembling of System Matrix

The frame has six DOF which include the displacements and rotations at the joints B and C. The member stiffness matrices are added up to obtain the system stiffness matrix (global coordinate). The relative contributions of the members AB, BC, and DC to the global stiffness is displayed in Figure 28. The system stiffness matrix can be written numerically as in Equations 47 and 48 [56].
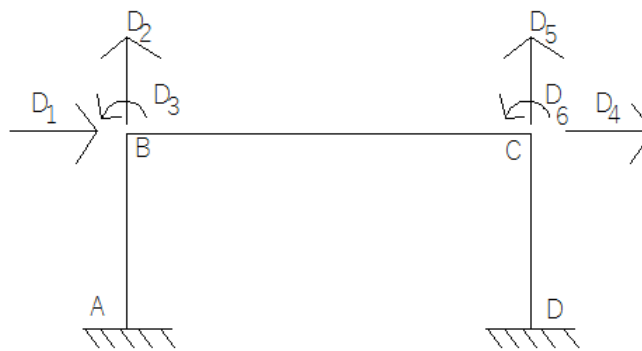
Figure 28. DOF of frame and global displacements, Case 3

$$K = \begin{bmatrix} k_{AB}^{44}+k_{BC}^{11} & k_{AB}^{45}+k_{BC}^{12} & k_{AB}^{46}+k_{BC}^{13} & k_{BC}^{14} & k_{BC}^{15} & k_{BC}^{16} \\ k_{AB}^{45}+k_{BC}^{12} & k_{AB}^{55}+k_{BC}^{22} & k_{AB}^{56}+k_{BC}^{23} & k_{BC}^{24} & k_{BC}^{25} & k_{BC}^{26} \\ k_{AB}^{46}+k_{BC}^{13} & k_{AB}^{56}+k_{BC}^{23} & k_{AB}^{66}+k_{BC}^{33} & k_{BC}^{34} & k_{BC}^{35} & k_{BC}^{36} \\ k_{BC}^{14} & k_{BC}^{24} & k_{BC}^{34} & k_{BC}^{44}+k_{DC}^{44} & k_{BC}^{45}+k_{DC}^{45} & k_{BC}^{46}+k_{DC}^{46} \\ k_{BC}^{15} & k_{BC}^{25} & k_{BC}^{35} & k_{BC}^{45}+k_{DC}^{45} & k_{BC}^{55}+k_{DC}^{55} & k_{BC}^{56}+k_{DC}^{56} \\ k_{BC}^{16} & k_{BC}^{26} & k_{BC}^{36} & k_{BC}^{46}+k_{DC}^{46} & k_{BC}^{56}+k_{DC}^{56} & k_{BC}^{66}+k_{DC}^{66} \end{bmatrix} \tag{47}$$

$$K = \begin{bmatrix} 324375 & 0 & 24750 & -312000 & 0 & 0 \\ 0 & 478641 & 13653 & 0 & -3641 & 13653 \\ 24750 & 13653 & 134267 & 0 & -13653 & 34133 \\ -312000 & 0 & 0 & 324375 & 0 & 24750 \\ 0 & -3641 & -13653 & 0 & 47841 & -13653 \\ 0 & 13653 & 34133 & 24750 & -13653 & 13427 \end{bmatrix} \tag{48}$$

3.3.4. Derivation of System Displacements

Employing the calculated system stiffness matrix and fixed end forces (force vector) and substituting in Equation 22, the joint displacements in the global coordinates are obtained in Equation 49.

$$
\begin{bmatrix}
324375 & 0 & 24750 & -312000 & 0 & 0 \\
0 & 478641 & 13653 & 0 & -3641 & 13653 \\
24750 & 13653 & 134267 & 0 & -13653 & 34133 \\
-312000 & 0 & 0 & 324375 & 0 & 24750 \\
0 & -3641 & -13653 & 0 & 47841 & -13653 \\
0 & 13653 & 34133 & 24750 & -13653 & 13427
\end{bmatrix}
\begin{Bmatrix} D_1 \\ D_2 \\ D_3 \\ D_4 \\ D_5 \\ D_6 \end{Bmatrix}
=
\begin{Bmatrix} 0 \\ -9 \\ -13.2 \\ 0 \\ -9 \\ 13.2 \end{Bmatrix};
\begin{Bmatrix} D_1 \\ D_2 \\ D_3 \\ D_4 \\ D_5 \\ D_6 \end{Bmatrix}
=
\begin{Bmatrix} 5.176666 \times 10^{-6} \\ -0.0000189474 \\ -0.000133103 \\ -5.176666 \times 10^{-6} \\ -0.0000189474 \\ 0.000133103 \end{Bmatrix}
\tag{49}
$$

3.3.5. Calculation of Member Forces

The derived system joint displacements are thus transformed into the local coordinates according to the numbering configuration of the frame structure at the global coordinate (Figure 29). However, these member displacements are substituted in Equations 22 and 27 to determine the member forces, as depicted in Figure 30 and Equations 50–52 for the members AB, BC, and DC, respectively [57].

$$
d_{AB}
\begin{Bmatrix} 0 \\ 0 \\ 0 \\ 5.176666 \times 10^{-6} \\ -0.0000189474 \\ -0.000133103 \end{Bmatrix}
\quad
d_{BC}
\begin{Bmatrix} 5.176666 \times 10^{-6} \\ -0.0000189474 \\ -0.000133103 \\ -5.176666 \times 10^{-6} \\ -0.0000189474 \\ 0.000133103 \end{Bmatrix}
\quad
d_{DC}
\begin{Bmatrix} 0 \\ 0 \\ 0 \\ 5.176666 \times 10^{-6} \\ -0.0000189474 \\ 0.000133103 \end{Bmatrix}
$$

Figure 29. Member displacements, Case 3
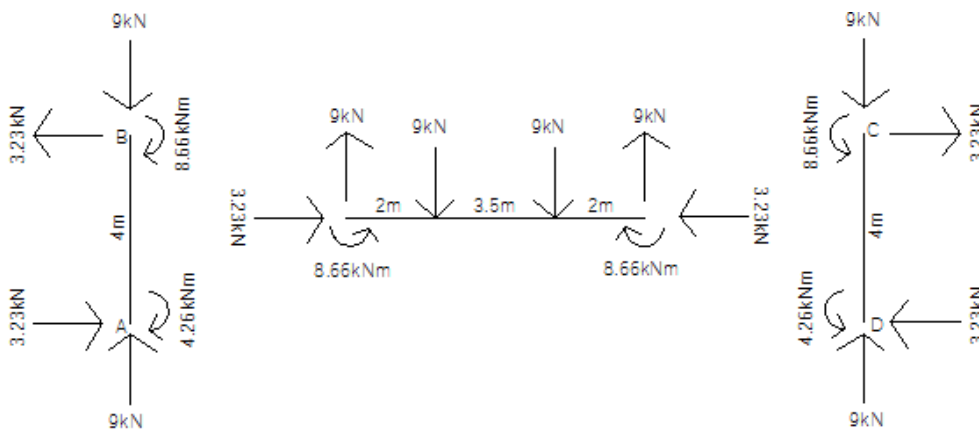
Figure 30. Member forces in free body diagram, Case 3

$$
\begin{Bmatrix} f_1 \\ f_2 \\ f_3 \\ f_4 \\ f_5 \\ f_6 \end{Bmatrix}
=
\begin{bmatrix}
12375 & 0 & -24750 & -12375 & 0 & -24750 \\
0 & 475000 & 0 & 0 & -475000 & 0 \\
-24750 & 0 & 66000 & 24750 & 0 & 33000 \\
-12375 & 0 & 24750 & 12375 & 0 & 24750 \\
0 & -475000 & 0 & 0 & 475000 & 0 \\
-24750 & 0 & 33000 & 24750 & 0 & 66000
\end{bmatrix}
\begin{Bmatrix} 0 \\ 0 \\ 0 \\ 5.176666 \times 10^{-6} \\ -0.0000189474 \\ -0.000133103 \end{Bmatrix}
=
\begin{Bmatrix} 3.23 \\ 9 \\ -4.26 \\ -3.23 \\ -9 \\ -8.66 \end{Bmatrix}
\tag{50}
$$

$$
\begin{Bmatrix} f_1 \\ f_2 \\ f_3 \\ f_4 \\ f_5 \\ f_6 \end{Bmatrix}
=
\begin{bmatrix}
312000 & 0 & 0 & 312000 & 0 & 0 \\
0 & 3641 & 13653 & 0 & -3641 & 13653 \\
0 & 13653 & 68267 & 0 & -13653 & 34133 \\
312000 & 0 & 0 & 312000 & 0 & 0 \\
0 & -3641 & -13653 & 0 & 3641 & -13653 \\
0 & 13653 & 34133 & 0 & -13653 & 68267
\end{bmatrix}
\begin{Bmatrix} 5.176666 \times 10^{-6} \\ -0.0000189474 \\ -0.000133103 \\ -5.176666 \times 10^{-6} \\ -0.0000189474 \\ 0.000133103 \end{Bmatrix}
+
\begin{Bmatrix} 0 \\ -9 \\ -13.2 \\ 0 \\ -9 \\ 13.2 \end{Bmatrix}
=
\begin{Bmatrix} 3.23 \\ 9 \\ 8.66 \\ -3.23 \\ 9 \\ -8.66 \end{Bmatrix}
\tag{51}
$$

$$
\begin{Bmatrix} f_1 \\ f_2 \\ f_3 \\ f_4 \\ f_5 \\ f_6 \end{Bmatrix}
=
\begin{bmatrix}
12375 & 0 & -24750 & -12375 & 0 & -24750 \\
0 & 475000 & 0 & 0 & -475000 & 0 \\
-24750 & 0 & 66000 & 24750 & 0 & 33000 \\
-12375 & 0 & 24750 & 12375 & 0 & 24750 \\
0 & -475000 & 0 & 0 & 475000 & 0 \\
-24750 & 0 & 33000 & 24750 & 0 & 66000
\end{bmatrix}
\begin{Bmatrix} 0 \\ 0 \\ 0 \\ 5.176666 \times 10^{-6} \\ -0.0000189474 \\ 0.000133103 \end{Bmatrix}
=
\begin{Bmatrix} -3.23 \\ 9 \\ 4.26 \\ 3.23 \\ -9 \\ 8.66 \end{Bmatrix}
\tag{52}
$$

4. Results and Discussion

The beam-column element stiffness matrix was derived in this analytical study by the superposition of the truss and beam elements stiffness matrices to statically analyze indeterminate MDOF frames. Through the application of this derived matrix stiffness method, the three internal stresses, namely the bending moments and shear and axial forces, are computed, which are necessary to evaluate the effects of applied concentrated and distributed loads on statically indeterminate structures. To actualize this benefit, three parametric studies, which are frames with varying geometries subjected to joint and member loads, were examined for the technical emphasis in this study using the finite element stiffness matrix approach. The study is relevant to the application of the derived six-coefficient stiffness matrix to determine the three internal stresses of the bending moments and shear and axial forces at both ends of the members elements. This analytical approach was also synthesized in the MATLAB software to ensure the accurate computation and analysis of indeterminate frame structures [58].

The first parametric study (Case 1) involves an indeterminate inverted L-shaped frame subjected to joint concentrated load and moment values of 20 kN and 10 kNm, respectively. Taking the provided sectional and geometry properties of the structure, the stiffness matrices for the connecting frame members were derived. The applied loads were used to formulate the fixed end forces in line with the numbering sequence and orientation of the four global DOF. The developed frame members' stiffness matrices were assembled to form the global stiffness matrix corresponding to the global DOF, taking the relationships between the six DOF of the beam-column element in the local coordinates into consideration. The assembled global stiffness matrix and the force vector, also known as fixed end forces, were utilized in the force-stiffness-displacement relationship to determine the system displacements, which are $D_1 = 0.00102$ m, $D_2 = 0.000163$ m, $D_3 = 0.00102$ m, and $D_4 = -0.0021$ m. The member forces are then determined by first localizing the computed global displacements and then plugging back the derived member stiffness matrix values in the force-stiffness-displacement formula. The calculated frame member forces showed that the effect of the joint forces on the inverted L-shaped frame resulted in a compressive axial force of 20.373 kN on the horizontal member with a clockwise moment of 6.266 kNm and 3.130 kNm on the left and right ends, respectively, and a tension force of 1.174 kN on the vertical members.

The Case 2 frame is also an inverted L-shaped similar to Case 1, subjected to a uniformly distributed load of 3 kN/m on the vertical member and a concentrated load of 16 kN on the horizontal member. The frame members' stiffness matrices were also calculated with the aid of their sectional and geometry properties. The subjected member loads on the frame structure were converted to fixed end forces using the associated formula and further transformed to the equivalent force vectors employing the force transformation matrix (Q). Similar to Case 1, the calculated frame members' stiffness matrices were assembled to form the global stiffness matrix corresponding to the global DOF, considering the relationships between the six DOF of the beam-column element in the local coordinates. The global stiffness matrix and the computed force vector were taken into the force-stiffness-displacement formula to calculate the system displacements, which are $D_1 = -0.00981$ m, $D_2 = 0.0000838$ m, $D_3 = -0.000136$ m, and $D_4 = 0.00293$ m. The member forces were determined by first transforming the computed global displacements to the local coordinates and then analyzing the values with the aid of the force-stiffness-displacement formula. The computed results indicated compressive forces of 10.47 kN and 13.63 kN for the horizontal and vertical frame members, respectively. Moreover, there was a clockwise moment of 11.68 kNm on the left end and an anticlockwise moment of 10.47 kNm on the right end of the horizontal member [59].

Lastly, Case 3 is a one-bay frame structure with two columns (vertical members) and connected with one horizontal member which is subjected to two concentrated loads of 9 kN at distance 2 m each from the ends and 3.5 m apart. The members' stiffness matrices were derived with the aid of the provided members' flexural rigidity and cross-sectional area, after which the applied loads were analyzed and transformed to fixed end forces employing the associated formula. Furthermore, the calculated members' stiffness matrices were assembled to achieve the global stiffness matrix conforming to the global DOF through the relationships between the beam-column element's six DOF in the local coordinates. The global stiffness matrix and the computed force vector were taken in the force-stiffness-displacement formula to calculate the system displacements which are $D_1 = 5.176666 \times 10^{-6}$ m, $D_2 = -0.0000189474$ m, $D_3 = -0.000133103$ m, $D_4 = 5.176666 \times 10^{-6}$ m, $D_5 = -0.0000189474$ m, and $D_6 = -0.000133103$ m. The member forces were determined by transforming the computed global displacements to the local coordinates and then analyzing the values with the aid of the force-stiffness-displacement formula. The computed results demonstrated compressive forces of 9 kN and 3.23 kN for the vertical and horizontal members, respectively. In addition, an anticlockwise moment of 8.66 kNm was calculated for the horizontal member, while clockwise and anticlockwise moments of 8.66 kNm and 3.23 kNm were respectively computed for the vertical members. Based on the derived results it can be concluded that the proposed finite element model and methodology can accurately determine the internal forces of MDOF frames. This is consistent with previous studies such as Gao [21], Zhou et al. [22], and Panahi and Zahrai [38] which also applied FEA to assess the behavior of MDOF frames under different loading conditions. Overall, the derived internal stresses revealed that the shear force values for the horizontal members were the axial forces in the vertical members and vice versa. The present study contributes to the understanding of the behavior of MDOF frames and provide valuable information for the design and analysis of such structures which is in consonance with the numerical analysis findings of Lou et al. [35] and Nukala and White [19].

4.1. Validation of Computed Results using SAP2000

The computational steps of the structural analysis for the three studied cases were synthesized in the MATLAB software to enable the flexible application of the formula method [36]. Using SAP2000, the three cases deployed for the parametric studies were modeled and analyzed. The obtained reactions (the bending moments and shear and axial forces) diagrams for the frames under the study in Cases 1–3 are presented in Figures 31–33, respectively [60]. One of the benefits of deploying SAP2000 for the frame analysis is its ability to perform parametric study which allows users to investigate the effects of different design parameters such as section properties and member sizes on the structural response. This feature is particularly useful for the optimization of the design and ensuring that the structure meets the required performance criteria. The models were first created in SAP2000 by defining the geometry and material properties and boundary conditions, the next step was the definition of loads applied to the structure, and then the analysis of the structure utilizing the FEM solver. The analysis would help calculate the internal forces and deformation of the structure under the applied loads [61, 62]. The derived results from SAP2000 were compared statistically with the reactions calculated with the beam-column element matrix formula which are listed in Table 1 and using the analysis of variance (ANOVA) approach to evaluate the statistical significance between the compared sets of data. The ANOVA results are summarized in Tables 2–4 for Cases 1–3, respectively [63, 64].
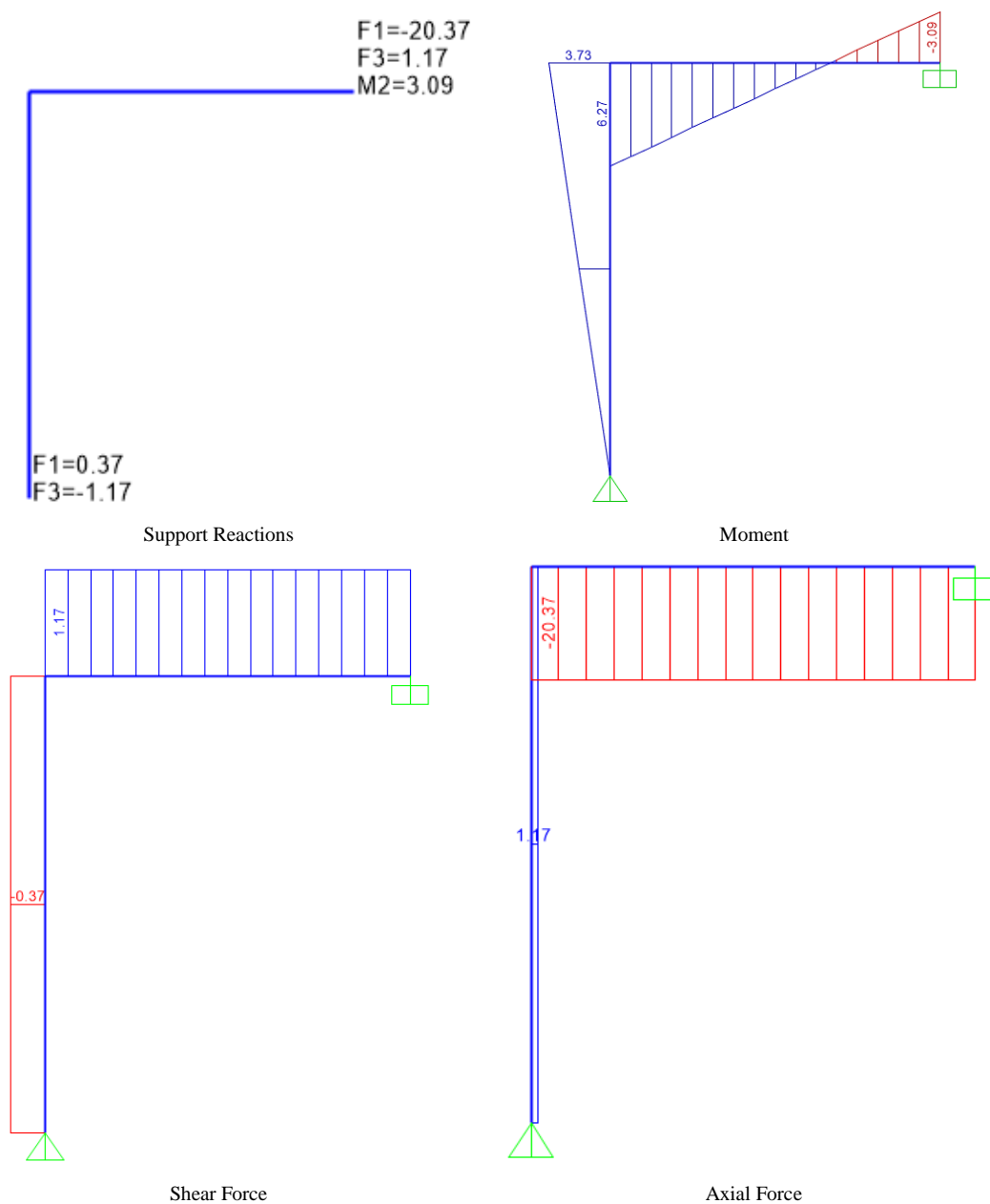

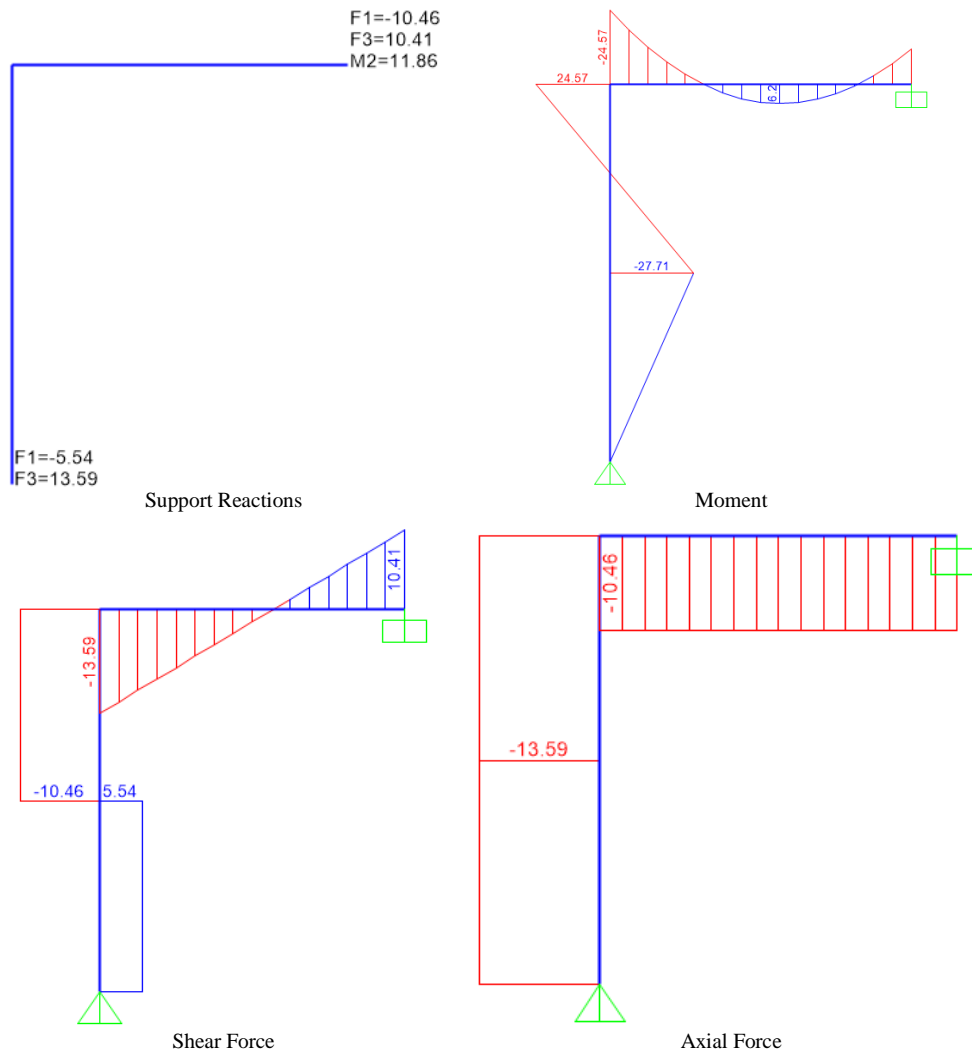
Figure 31. SAP2000 analysis results for Case 1

Figure 32. SAP2000 analysis results for Case 2
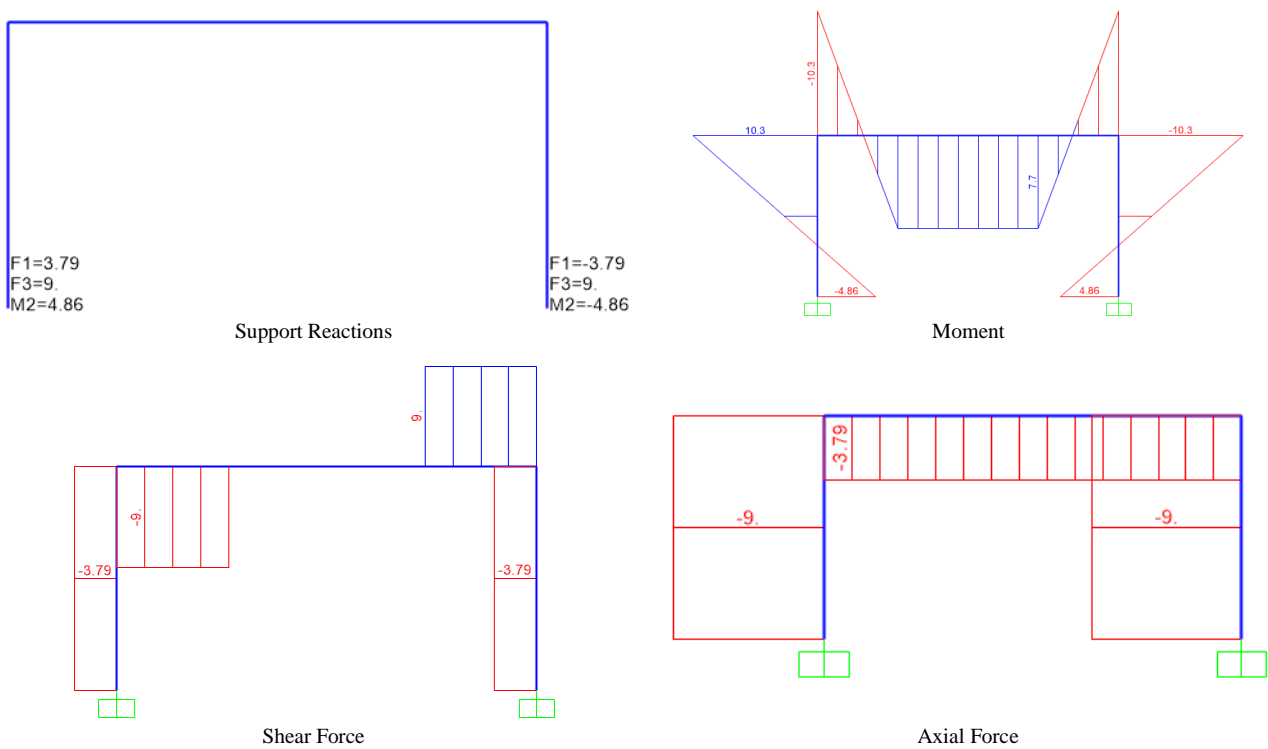
Figure 33. SAP2000 analysis results for Case 3

Table 1. Calculated results compared with SAP2000 analysis results

Case 1		
Internal Forces	**Calculated Results**	**SAP2000**
Shear-AB[1]	0.373	0.37
Axial-AB[1]	-1.174	-1.17
BM-AB[1]	0	0
Shear-AB[2]	-3.373	-0.37
Axial-AB[2]	1.174	1.17
BM-AB[2]	-3.734	-3.73
Shear-BC[1]	-1.174	-1.17
Axial-BC[1]	20.373	20.37
BM-BC[1]	-6.266	-6.27
Shear-BC[2]	1.174	1.17
Axial-BC[2]	-20.373	-20.37
BM-BC[2]	-3.13	-3.09
Case 2		
Internal Forces	**Calculated Results**	**SAP2000**
Shear-AB[1]	-5.53	-5.54
Axial-AB[1]	13.63	13.59
BM-AB[1]	0	0
Shear-AB[2]	-10.47	-10.46
Axial-AB[2]	13.63	-13.59
BM-AB[2]	24.71	-24.57
Shear-BC[1]	13.63	13.59
Axial-BC[1]	10.47	10.46
BM-BC[1]	24.71	24.57
Shear-BC[2]	10.37	10.41
Axial-BC[2]	-10.47	-10.46
BM-BC[2]	-11.68	-11.86
Case 3		
Internal Forces	**Calculated Results**	**SAP2000**
Shear-AB[1]	3.23	3.79
Axial-AB[1]	9	9
BM-AB[1]	-4.26	-4.86
Shear-AB[2]	-3.23	-3.79
Axial-AB[2]	-9	-9
BM-AB[2]	-8.66	-10.3
Shear-BC[1]	9	9
Axial-BC[1]	3.23	3.79
BM-BC[1]	8.66	10.3
Shear-BC[2]	9	9
Axial-BC[2]	-3.23	-3.79
BM-BC[2]	8.66	10.3
Shear-DC[1]	-3.23	-3.79
Axial-DC[1]	9	9
BM-DC[1]	4.26	4.86
Shear-DC[2]	3.23	3.79
Axial-DC[2]	-9	-9
BM-DC[2]	8.66	10.3

BM = bending moment; superscripts 1 and 2 indicate member nodes.

Table 2. ANOVA results for Case 1

Groups	Count	Sum	Average	Variance		
Calculated result	12	-16.13	-1.34417	80.76987		
SAP2000	12	-13.09	-1.09083	80.37437		
Source of Variation	**SS**	**df**	**MS**	**F**	**P-value**	**F$_{crit}$**
Between Groups	0.385067	1	0.385067	0.004779	0.94551	4.30095
Within Groups	1772.587	22	80.57212			
Total	1772.972	23				

Table 3. ANOVA results for Case 2

Groups	Count	Sum	Average	Variance		
Calculated result	12	73	6.083333	176.1653		
SAP2000	12	-3.86	-0.32167	215.2861		
Source of Variation	**SS**	**df**	**MS**	**F**	**P-value**	**F$_{crit}$**
Between Groups	246.1442	1	246.1442	1.257598	0.274198	4.30095
Within Groups	4305.965	22	195.7257			
Total	4552.109	23				

Table 4. ANOVA results for Case 3

Groups	Count	Sum	Average	Variance		
Calculated result	18	35.32	1.962222	47.97467		
SAP2000	18	38.6	2.144444	56.5299		
Source of Variation	**SS**	**df**	**MS**	**F**	**P-value**	**F$_{crit}$**
Between Groups	0.298844	1	0.298844	0.005719	0.94016	4.130018
Within Groups	1776.578	34	52.25228			
Total	1776.876	35				

The obtained statistical results displayed that the calculated P-value was greater than the critical value of 0.05, with the calculated scores of 0.94551, 0.274198, and 0.94016 for Cases 1, 2, and 3, respectively, which signified that there is no significant difference between the sets of data under the investigation. The statistical analysis helps affirm the accuracy and performance of the computed results using the beam-column element matrix formula when compared with the analysis outcomes derived from SAP2000 [50, 65].

5. Conclusions

The application of the stiffness matrix approach to finite elements was investigated in this study on indeterminate structures. The following conclusions can be drawn from the obtained results:

- The study on the analysis of frame structures using FEM presents a convenient and systematic approach for analyzing the behavior of frame structures under different loading conditions, and the results achieved from the analysis can be used to design more efficient and cost-effective frame structures.

- The superposition of the truss and beam elements stiffness matrices in order to formulate the member stiffness matrix of a beam-column element with six DOF at each of the two nodes of the member was essentially addressed to provide foundational background on the derivation and application of FEM.

- The deployment of this matrix approach to analyze indeterminate frame structures with joint and member loads was further examined to derive the reactions (bending moments and shear and axial forces), and the computed results showed that the proposed approach was effective in predicting the internal forces in frame members.

- For the purpose of emphasis, this matrix approach was used to analyze three different parametric study cases that featured frame structures with varying geometries and loading conditions. This was done to assess the adaptability and suitability of this formula for the analysis of indeterminate frames. The accuracy of the results was verified through comparison with previous studies, which demonstrated that the beam-column element was suitable for analyzing the behavior of frame structures.

- In order to evaluate the performance of this method, the results derived from the element stiffness matrix approach were compared with the results obtained from the finite element software (SAP2000) using the analysis of variance (ANOVA). The statistical results indicated a good correlation between the compared results with a P-value > 0.05 to uncover the adequate performance for the derived beam-column element matrix formula method.

- The study can contribute to the new knowledge in the field of structural engineering by presenting a practical approach for determining the internal forces in frame structures subjected to different loads compared with the traditional methods. This method can be used by engineers to optimize the design and analysis of frame structures for various applications such as buildings, bridges, and other infrastructural projects to improve their performance.

6. Abbreviations and Parameters

Q	Force transformation matrix	T	Displacement transformation matrix
D_i	System displacements	d_i	Local displacements
E	Modulus of elasticity of material	I	Moment of inertia about axis of bending
A	Cross-sectional area of material	k	Member stiffness matrix
f_i	Member force vector	DOF	Degrees of freedom
F_i	Global force	FEM	Finite element method
MDOF	Multiple degrees-of-freedom	k_T	Truss element stiffness matrix
FEA	Finite element analysis	l	Span length
k_B	Beam element stiffness matrix	w	Uniformly distributed load
p	Concentrated applied load		

7. Declarations

7.1. Author Contributions

Conceptualization, G.U.A. A.B., O.N.O., B.O.I., and E.A.O.; methodology, G.U.A., A.B., and U.I.I.; validation, G.U.A., A.B., N.G., and R.C.U.; formal analysis, G.U.A., A.B., O.N.O., B.O.I., and E.A.O.; investigation, G.U.A., A.B., and R.C.U.; resources, A.B.; data curation, G.U.A., A.B., and B.O.I.; writing—original draft preparation, A.B., O.N.O., and R.C.U.; writing—review and editing, G.U.A., A.B., and U.I.I.; visualization, A.B., U.I.I., N.G., and E.A.O.; project administration, A.B. and U.I.I. All authors have read and agreed to the published version of the manuscript.

7.2. Data Availability Statement

Data sharing is not applicable to this article.

7.3. Funding

The authors received no financial support for the research, authorship, and/or publication of this article.

7.4. Conflicts of Interest

The authors declare no conflict of interest.

8. References

[1] Xu, Q., Zhen, X., Zhang, Y., Han, M., & Zhang, W. (2022). Numerical simulation study of progressive collapse of reinforced concrete frames with masonry infill walls under blast loading. Modelling and Simulation in Engineering, 2022. doi:10.1155/2022/1781415.

[2] Fu, F. (2013). Dynamic response and robustness of tall buildings under blast loading. Journal of Constructional steel research, 80, 299-307. doi:10.1016/j.jcsr.2012.10.001.

[3] Rao, S. S. (2017). The finite element method in engineering. Butterworth-heinemann, Oxford, United Kingdom.

[4] Kattner, M., & Crisinel, M. (2000). Finite element modelling of semi-rigid composite joints. Computers and Structures, 78(1), 341–353. doi:10.1016/S0045-7949(00)00064-X.

[5] Anuntasena, W., Lenwari, A., & Thepchatri, T. (2019). Finite element modelling of concrete-encased steel columns subjected to eccentric loadings. Engineering Journal, 23(6), 299–310. doi:10.4186/ej.2019.23.6.299.

[6] Wang, M., Shi, Y., Xu, J., Yang, W., & Li, Y. (2015). Experimental and numerical study of unstiffened steel plate shear wall structures. Journal of Constructional Steel Research, 112, 373-386. doi:10.1016/j.jcsr.2015.05.002.

[7] Pepper, D. W., & Heinrich, J. C. (2005). The finite element method: basic concepts and applications. CRC Press, Boca Raton, United States.

[8] Öchsner, A. (2016). Computational statics and dynamics: An introduction based on the finite element method. Springer, Singapore. doi:10.1007/978-981-10-0733-0.

[9] Öchsner, A., & Merkel, M. (2018). One-dimensional finite elements: An introduction to the FE method. Springer, Cham, Switzerland. doi:10.1007/978-3-319-75145-0.

[10] Zienkiewicz, O. C., & Taylor, R. L. (2000). The finite element method: solid mechanics (Volume 2). Butterworth-Heinemann, Oxford, United Kingdom.

[11] Pelosi, G. (2007). The finite-element method, Part I: R. L. Courant "Historical Corner". IEEE Antennas and Propagation Magazine, 49(2), 180–182. doi:10.1109/map.2007.376627.

[12] Huebner, K. H., Dewhirst, D. L., Smith, D. E., & Byrom, T. G. (2001). The finite element method for engineers. John Wiley & Sons, Hoboken, United States.

[13] Pathak, M. V., & Bhaskar, G. B. (2016). Finite element analysis program of frames. International Journal for Technological Research in Engineering, 3(9), 2455–2459.

[14] Alaneme, G. U., Ezeokpube, G. C., & Mbadike, E. M. (2020). Failure analysis of a partially collapsed building using analytical hierarchical process. Journal of Failure Analysis and Prevention. doi:10.1007/s11668-020-01040-3.

[15] Rahemi, H., & Baksh, S. (2010). Finite difference impulsive response analysis of a frame structure-a Matlab computational project-based learning. Latin American and Caribbean Journal of Engineering Education, 4(2), 31-38.

[16] Madenci, E., & Guven, I. (2015). The finite element method and applications in engineering using ANSYS®. Springer, New York, United States. doi:10.1007/978-1-4899-7550-8.

[17] Cao, J. (2005). Application of a posteriori error estimation to finite element simulation of compressible Navier-Stokes flow. Computers and Fluids, 34(8), 991–1024. doi:10.1016/j.compfluid.2004.09.002.

[18] Kattan, P. I. (2010). MATLAB guide to finite elements: an interactive approach. Springer Science & Business Media, Berlin, Germany. doi:10.1007/978-3-540-70698-4.

[19] Nukala, P. K. V. V., & White, D. W. (2004). A mixed finite element for three-dimensional nonlinear analysis of steel frames. Computer Methods in Applied Mechanics and Engineering, 193(23–26), 2507–2545. doi:10.1016/j.cma.2004.01.029.

[20] Li, Y., Lu, X., Guan, H., & Ren, P. (2016). Numerical investigation of progressive collapse resistance of reinforced concrete frames subject to column removals from different stories. Advances in Structural Engineering, 19(2), 314–326. doi:10.1177/1369433215624515.

[21] Gao, Y. (2021). Seismic Performance Simulation of Magnetorheological Fluid Dampers with Single Degree-of-Freedom System. University of California, Irvine, United States.

[22] Zhou, X., Chen, Y., Ke, K., Yam, M. C., & Li, H. (2022). Hybrid steel staggered truss frame (SSTF): A probabilistic spectral energy modification coefficient surface model for damage-control evaluation and performance insights. Journal of Building Engineering, 45, 103556. doi:10.1016/j.jobe.2021.103556.

[23] Panahi, M., Zareei, S. A., & Izadi, A. (2021). Flexural strengthening of reinforced concrete beams through externally bonded FRP sheets and near surface mounted FRP bars. Case Studies in Construction Materials, 15, e00601. doi:10.1016/j.cscm.2021.e00601.

[24] Fujii, K. (2014). Prediction of the largest peak nonlinear seismic response of asymmetric buildings under bi-directional excitation using pushover analyses. Bulletin of Earthquake Engineering, 12, 909-938. doi:10.1007/s10518-013-9557-x.

[25] Liew, J. R. (2008). Survivability of steel frame structures subject to blast and fire. Journal of Constructional Steel Research, 64(7-8), 854-866. doi:10.1016/j.jcsr.2007.12.013.

[26] Khalid, M. A., & Bansal, S. (2023). Framework for robust design optimization of tuned mass dampers by stochastic subset optimization. International Journal of Structural Stability and Dynamics, 2350155. doi:10.1142/S0219455423501559.

[27] Ganjavi, B., & Hao, H. (2012). A parametric study on the evaluation of ductility demand distribution in multi-degree-of-freedom systems considering soil–structure interaction effects. Engineering Structures, 43, 88-104. doi:10.1016/j.engstruct.2012.05.006.

[28] Ainsworth, M., & Oden, J. T. (2000). A Posteriori Error Estimation in Finite Element Analysis. John Wiley & Sons, Hoboken, United States. doi:10.1002/9781118032824.

[29] Qiu, C., Zhang, A., Jiang, T., & Du, X. (2022). Seismic performance analysis of multi-story steel frames equipped with FeSMA BRBs. Soil Dynamics and Earthquake Engineering, 161, 107392. doi:10.1016/j.soildyn.2022.107392.

[30] Yussof, M. M., Silalahi, J. H., Kamarudin, M. K., Chen, P.-S., & Parke, G. A. (2020). Numerical evaluation of dynamic responses of steel frame structures with different types of haunch connection under blast load. Applied Sciences, 10(5), 1815. doi:10.3390/app10051815.

[31] Khaloo, A. R., & Khosravi, H. (2013). Modified fish-bone model: A simplified MDOF model for simulation of seismic responses of moment resisting frames. Soil Dynamics and Earthquake Engineering, 55, 195-210. doi:10.1016/j.soildyn.2013.09.013.

[32] Muho, E. V., Qian, J., & Beskos, D. E. (2020). A direct displacement-based seismic design method using a MDOF equivalent system: application to R/C framed structures. Bulletin of Earthquake Engineering, 18, 4157-4188. doi:10.1007/s10518-020-00857-5.

[33] Ou, C., Liu, J., Sun, L., Xiao, Z., Cheng, Y., Liu, M., Zhao, F., Zhen, M., & Wang, Y. (2021). Experimental and Numerical Investigation on the Dynamic Responses of the Remaining Structure under Impact Loading with Column Being Removed. KSCE Journal of Civil Engineering, 25(6), 2078–2088. doi:10.1007/s12205-021-1026-5.

[34] Fragiacomo, M., Amadio, C., & Macorini, L. (2004). Seismic response of steel frames under repeated earthquake ground motions. Engineering Structures, 13(26), 2021-2035. doi:10.1016/j.engstruct.2004.08.005.

[35] Lou, P., Dai, G. L., & Zeng, Q. Y. (2006). Finite-element analysis for a Timoshenko beam subjected to a moving mass. Proceedings of the Institution of Mechanical Engineers, Part C: Journal of Mechanical Engineering Science, 220(5), 669–678. doi:10.1243/09544062JMES119.

[36] Diskin, B., & Thomas, J. (2012). Effects of mesh regularity on accuracy of finite-volume schemes. 50th AIAA Aerospace Sciences Meeting Including the New Horizons Forum and Aerospace Exposition. doi:10.2514/6.2012-609.

[37] Hjelmstad, K. D., & Taciroglu, E. (2002). Mixed methods and flexibility approaches for nonlinear frame analysis. Journal of Constructional Steel Research, 58(5–8), 967–993. doi:10.1016/S0143-974X(01)00100-6.

[38] Panahi, S., & Zahrai, S. M. (2021). Performance of typical plan concrete buildings under progressive collapse. Structures, 31, 1163-1172. doi:10.1016/j.istruc.2021.02.045.

[39] Shan, S., & Pan, W. (2022). Collapse mechanisms of multi-story steel-framed modular structures under fire scenarios. Journal of Constructional Steel Research, 196, 107419. doi:10.1016/j.jcsr.2022.107419.

[40] Ross, C. T. (1998). Advanced applied finite element methods. Woodhead, Sawston, United Kingdom. doi:10.1533/9780857099754.

[41] Shan, S., & Pan, W. (2020). Structural design of high‐rise buildings using steel‐framed modules: A case study in Hong Kong. The Structural Design of Tall and Special Buildings, 29(15), e1788. doi:10.1002/tal.1788.

[42] Van Loan, C. F., & Golub, G. (1996). Matrix computations. The Johns Hopkins University Press, Baltimore, United States.

[43] ASME PTC 60/V&V 10-2006 (2006) Guide for Verification and Validation in Computational Solid Mechanics. The American Society of Mechanical Engineers Standards, New York, United States.

[44] Spacone, E., Filippou, F. C., & Taucer, F. F. (1996). Fibre beam‐column model for non‐linear analysis of R/C frames: Part I. Formulation. Earthquake Engineering and Structural Dynamics, 25(7), 711-725. doi:10.1002/(SICI)1096-9845(199607)25:7<711::AID-EQE576>3.0.CO;2-9.

[45] Ross, C. T., & Chilver, A. (1999). Strength of materials and structures (4th Ed.). Elsevier, Amsterdam, Netherlands.

[46] Sharma, S., & Tiwary, A. K. (2021). Analysis of multi-story buildings with hybrid shear wall: steel bracing structural system. Innovative Infrastructure Solutions, 6, 1-12. doi:10.1007/s41062-021-00548-3.

[47] Horr, A. M., & Schmidt, L. C. (1995). Closed-form solution for the Timoshenko beam theory using a computer-based mathematical package. Computers and Structures, 55(3), 405–412. doi:10.1016/0045-7949(95)98867-P.

[48] Ferreira, A. J. (2009). MATLAB codes for finite element analysis. Springer, Cham, Switzerland. doi:10.1007/978-3-030-47952-7.

[49] Agor, C. D., Mbadike, E. M., & Alaneme, G. U. (2023). Evaluation of sisal fiber and aluminum waste concrete blend for sustainable construction using adaptive neuro-fuzzy inference system. Scientific Reports, 13(1), 2814. doi:10.1038/s41598-023-30008-0.

[50] Rangel, R. L., & Martha, L. F. (2019). LESM—An object-oriented MATLAB program for structural analysis of linear element models. Computer Applications in Engineering Education, 27(3), 553–571. doi:10.1002/cae.22097.

[51] Brenner, S. C., & Scott, L. R. (2008). The mathematical theory of finite element methods. Springer, New York, United States. doi:10.1007/978-0-387-75934-0.

[52] Ghali, A., Neville, A. M., & Brown, T. G. (2009). Structural analysis: a unified classical and matrix approach (6th Ed.). CRC Press, London, United Kingdom. doi:10.1201/9781315273006.

[53] Wunderlich, W., & Pilkey, W. D. (2004). Mechanics of structures. Variational and computational methods. Meccanica 39, 291–292. doi:10.1023/b:mecc.0000023038.64148.bc.

[54] Bathe, K. J. (1996). Finite element procedures. Prentice Hall, Koboken, United States.

[55] Trogrlic, B., & Mihanovic, A. (2008). The comparative body model in material and geometric nonlinear analysis of space R/C frames. Engineering Computations, 25(2), 155-171. doi:10.1108/02644400810855968.

[56] Timoshenko, S.P. & Goodier J. N. (1970). Theory of Elasticity (3rd Ed.), McGraw-Hill, New York, United States.

[57] Slivker, V. (2006). Mechanics of structural elements: theory and applications. Springer. doi:10.1007/978-3-540-44721-4.

[58] Zhang, X. D., Trépanier, J. Y., & Camarero, R. (2000). A posteriori error estimation for finite-volume solutions of hyperbolic conservation laws. Computer Methods in Applied Mechanics and Engineering, 185(1), 1–19. doi:10.1016/S0045-7825(99)00099-7.

[59] Najafgholipour, M. A., Dehghan, S. M., Dooshabi, A., & Niroomandi, A. (2017). Finite element analysis of reinforced concrete beam-column connections with governing joint shear failure mode. Latin American Journal of Solids and Structures, 14(7), 1200–1225. doi:10.1590/1679-78253682.

[60] Duan, H., & Hueste, M. B. D. (2012). Seismic performance of a reinforced concrete frame building in China. Engineering Structures, 41, 77-89. doi:10.1016/j.engstruct.2012.03.030.

[61] Shi, F., Wang, H., Zong, L., Ding, Y., & Su, J. (2020). Seismic behavior of high-rise modular steel constructions with various module layouts. Journal of Building Engineering, 31, 101396. doi:10.1016/j.jobe.2020.101396.

[62] Lopes, P. C., Rangel, R. L., & Martha, L. F. (2021). An interactive user interface for a structural analysis software using computer graphics techniques in MATLAB. Computer Applications in Engineering Education, 29(6), 1505–1525. doi:10.1002/cae.22406.

[63] Ibe Iro, U., Alaneme, G. U., Milad, A., Olaiya, B. C., Otu, O. N., Isu, E. U., & Amuzie, M. N. (2022). Optimization and simulation of saw dust ash concrete using extreme vertex design method. Advances in Materials Science and Engineering, 2022. doi:10.1155/2022/5082139.

[64] Attah, I. C., Kufre Etim, R., Uwadiegwu Alaneme, G., Ufot Ekpo, D., & Usanga, I. N. (2022). Scheffe's approach for single additive optimization in selected soils amelioration studies for cleaner environment and sustainable subgrade materials. Cleaner Materials, 5. doi:10.1016/j.clema.2022.100126.

[65] Alaneme George, U., & Mbadike Elvis, M. (2019). Modelling of the mechanical properties of concrete with cement ratio partially replaced by aluminium waste and sawdust ash using artificial neural network. SN Applied Sciences, 1(11), 1514. doi:10.1007/s42452-019-1504-2.